International Telecommunication Union

ITU-R

Radiocommunication Sector of ITU

Recommendation ITU-R P.530-14
(02/2012)

Propagation data and prediction methods required for the design of terrestrial line-of-sight systems

P Series
Radiowave propagation

Foreword

The role of the Radiocommunication Sector is to ensure the rational, equitable, efficient and economical use of the radio-frequency spectrum by all radiocommunication services, including satellite services, and carry out studies without limit of frequency range on the basis of which Recommendations are adopted.

The regulatory and policy functions of the Radiocommunication Sector are performed by World and Regional Radiocommunication Conferences and Radiocommunication Assemblies supported by Study Groups.

Policy on Intellectual Property Right (IPR)

ITU-R policy on IPR is described in the Common Patent Policy for ITU-T/ITU-R/ISO/IEC referenced in Annex 1 of Resolution ITU-R 1. Forms to be used for the submission of patent statements and licensing declarations by patent holders are available from http://www.itu.int/ITU-R/go/patents/en where the Guidelines for Implementation of the Common Patent Policy for ITU-T/ITU-R/ISO/IEC and the ITU-R patent information database can also be found.

Series of ITU-R Recommendations

(Also available online at http://www.itu.int/publ/R-REC/en)

Series	Title
BO	Satellite delivery
BR	Recording for production, archival and play-out; film for television
BS	Broadcasting service (sound)
BT	Broadcasting service (television)
F	Fixed service
M	Mobile, radiodetermination, amateur and related satellite services
P	**Radiowave propagation**
RA	Radio astronomy
RS	Remote sensing systems
S	Fixed-satellite service
SA	Space applications and meteorology
SF	Frequency sharing and coordination between fixed-satellite and fixed service systems
SM	Spectrum management
SNG	Satellite news gathering
TF	Time signals and frequency standards emissions
V	Vocabulary and related subjects

Note: *This ITU-R Recommendation was approved in English under the procedure detailed in Resolution ITU-R 1.*

Electronic Publication
Geneva, 2012

RECOMMENDATION ITU-R P.530-14

Propagation data and prediction methods required for the design of terrestrial line-of-sight systems

(Question ITU-R 204/3)

(1978-1982-1986-1990-1992-1994-1995-1997-1999-2001-2001-2005-2007-2009-2012)

Scope

This Recommendation provides prediction methods for the propagation effects that should be taken into account in the design of digital fixed line-of-sight links, both in clear-air and rainfall conditions. It also provides link design guidance in clear step-by-step procedures including the use of mitigation techniques to minimize propagation impairments. The final outage predicted is the base for other Recommendations addressing error performance and availability.

The ITU Radiocommunication Assembly,

considering

a) that for the proper planning of terrestrial line-of-sight systems it is necessary to have appropriate propagation prediction methods and data;

b) that methods have been developed that allow the prediction of some of the most important propagation parameters affecting the planning of terrestrial line-of-sight systems;

c) that as far as possible these methods have been tested against available measured data and have been shown to yield an accuracy that is both compatible with the natural variability of propagation phenomena and adequate for most present applications in system planning,

recommends

1 that the prediction methods and other techniques set out in Annex 1 be adopted for planning terrestrial line-of-sight systems in the respective ranges of parameters indicated.

Annex 1

1 Introduction

Several propagation effects must be considered in the design of line-of-sight radio-relay systems. These include:

– diffraction fading due to obstruction of the path by terrain obstacles under adverse propagation conditions;

– attenuation due to atmospheric gases;

– fading due to atmospheric multipath or beam spreading (commonly referred to as defocusing) associated with abnormal refractive layers;

– fading due to multipath arising from surface reflection;

– attenuation due to precipitation or solid particles in the atmosphere;
– variation of the angle-of-arrival at the receiver terminal and angle-of-launch at the transmitter terminal due to refraction;
– reduction in cross-polarization discrimination (XPD) in multipath or precipitation conditions;
– signal distortion due to frequency selective fading and delay during multipath propagation.

One purpose of this Annex is to present in concise step-by-step form simple prediction methods for the propagation effects that must be taken into account in the majority of fixed line-of-sight links, together with information on their ranges of validity. Another purpose of this Annex is to present other information and techniques that can be recommended in the planning of terrestrial line-of-sight systems.

Prediction methods based on specific climate and topographical conditions within an administration's territory may be found to have advantages over those contained in this Annex.

With the exception of the interference resulting from reduction in XPD, the Annex deals only with effects on the wanted signal. Some overall allowance is made in § 2.3.6 for the effects of intra-system interference in digital systems, but otherwise the subject is not treated. Other interference aspects are treated in separate Recommendations, namely:

– inter-system interference involving other terrestrial links and earth stations in Recommendation ITU-R P.452;
– inter-system interference involving space stations in Recommendation ITU-R P.619.

To optimize the usability of this Annex in system planning and design, the information is arranged according to the propagation effects that must be considered, rather than to the physical mechanisms causing the different effects.

It should be noted that the term "worst month" used in this Recommendation is equivalent to the term "any month" (see Recommendation ITU-R P.581).

2 Propagation loss

The propagation loss on a terrestrial line-of-sight path relative to the free-space loss (see Recommendation ITU-R P.525) is the sum of different contributions as follows:

– attenuation due to atmospheric gases;
– diffraction fading due to obstruction or partial obstruction of the path;
– fading due to multipath, beam spreading and scintillation;
– attenuation due to variation of the angle-of-arrival/launch;
– attenuation due to precipitation;
– attenuation due to sand and dust storms.

Each of these contributions has its own characteristics as a function of frequency, path length and geographic location. These are described in the paragraphs that follow.

Sometimes propagation enhancement is of interest. In such cases it is considered following the associated propagation loss.

2.1 Attenuation due to atmospheric gases

Some attenuation due to absorption by oxygen and water vapour is always present, and should be included in the calculation of total propagation loss at frequencies above about 10 GHz. The attenuation on a path of length d (km) is given by:

$$A_a = \gamma_a \, d \qquad \text{dB} \tag{1}$$

The specific attenuation γ_a (dB/km) should be obtained using Recommendation ITU-R P.676.

NOTE 1 – On long paths at frequencies above about 20 GHz, it may be desirable to take into account known statistics of water vapour density and temperature in the vicinity of the path. Information on water vapour density is given in Recommendation ITU-R P.836.

2.2 Diffraction fading

Variations in atmospheric refractive conditions cause changes in the effective Earth's radius or k-factor from its median value of approximately 4/3 for a standard atmosphere (see Recommendation ITU-R P.310). When the atmosphere is sufficiently sub-refractive (large positive values of the gradient of refractive index, low k-factor values), the ray paths will be bent in such a way that the Earth appears to obstruct the direct path between transmitter and receiver, giving rise to the kind of fading called diffraction fading. This fading is the factor that determines the antenna heights.

k-factor statistics for a single point can be determined from measurements or predictions of the refractive index gradient in the first 100 m of the atmosphere (see Recommendation ITU-R P.453 on effects of refraction). These gradients need to be averaged in order to obtain the effective value of k for the path length in question, k_e. Values of k_e exceeded for 99.9% of the time are discussed in terms of path clearance criteria in the following section.

2.2.1 Diffraction loss dependence on path clearance

Diffraction loss will depend on the type of terrain and the vegetation. For a given path ray clearance, the diffraction loss will vary from a minimum value for a single knife-edge obstruction to a maximum for smooth spherical Earth. Methods for calculating diffraction loss for these two cases and also for paths with irregular terrain are discussed in Recommendation ITU-R P.526. These upper and lower limits for the diffraction loss are shown in Fig. 1.

The diffraction loss over average terrain can be approximated for losses greater than about 15 dB by the formula:

$$A_d = -20\, h / F_1 + 10 \qquad \text{dB} \tag{2}$$

where h is the height difference (m) between most significant path blockage and the path trajectory (h is negative if the top of the obstruction of interest is above the virtual line-of-sight) and F_1 is the radius of the first Fresnel ellipsoid given by:

$$F_1 = 17.3\sqrt{\frac{d_1 \, d_2}{f d}} \qquad \text{m} \tag{3}$$

with:

f: frequency (GHz)

d: path length (km)

d_1 and d_2: distances (km) from the terminals to the path obstruction.

A curve, referred to as A_d, based on equation (2) is also shown in Fig. 1. This curve, strictly valid for losses larger than 15 dB, has been extrapolated up to 6 dB loss to fulfil the need of link designers.

FIGURE 1

Diffraction loss for obstructed line-of-sight microwave radio paths

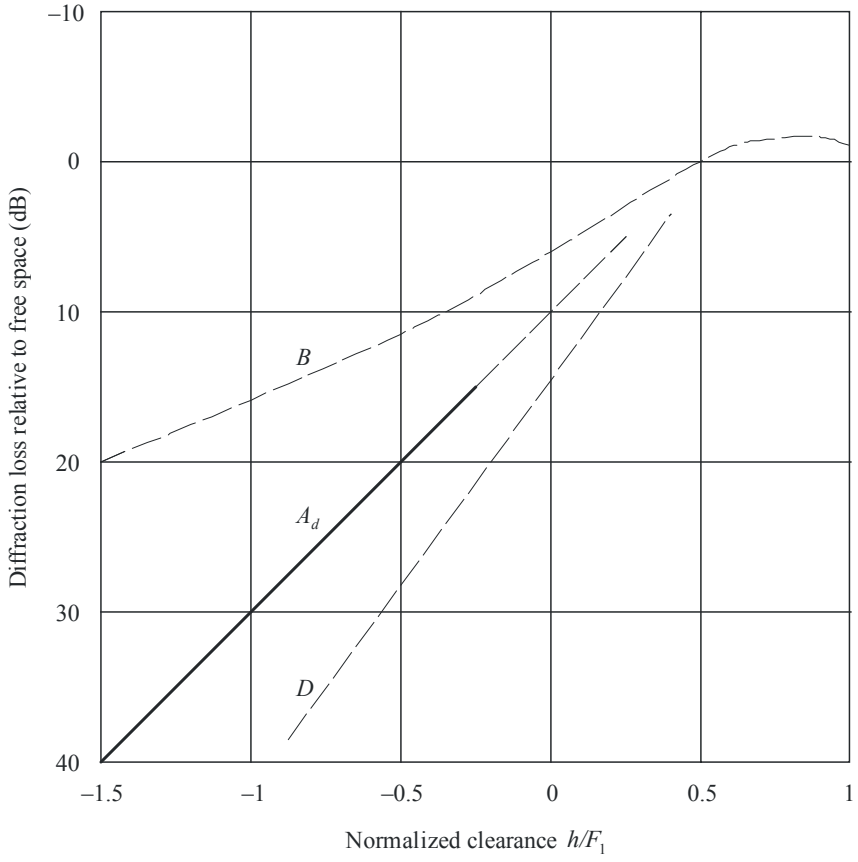

B: theoretical knife-edge loss curve
D: theoretical smooth spherical Earth loss curve, at 6.5 GHz and $k_e = 4/3$
A_d: empirical diffraction loss based on equation (2) for intermediate terrain
h: amount by which the radio path clears the Earth's surface
F_1: radius of the first Fresnel zone

P.0530-01

2.2.2 Planning criteria for path clearance

At frequencies above about 2 GHz, diffraction fading of this type has in the past been alleviated by installing antennas that are sufficiently high, so that the most severe ray bending would not place the receiver in the diffraction region when the effective Earth radius is reduced below its normal value. Diffraction theory indicates that the direct path between the transmitter and the receiver needs a clearance above ground of at least 60% of the radius of the first Fresnel zone to achieve free-space propagation conditions. Recently, with more information on this mechanism and the statistics of k_e that are required to make statistical predictions, some administrations are installing antennas at heights that will produce some small known outage.

In the absence of a general procedure that would allow a predictable amount of diffraction loss for various small percentages of time and therefore a statistical path clearance criterion, the following procedure is advised for temperate and tropical climates.

2.2.2.1 Non-diversity antenna configurations

Step 1: Determine the antenna heights required for the appropriate median value of the point k-factor (see § 2.2; in the absence of any data, use $k = 4/3$) and 1.0 F_1 clearance over the highest obstacle (temperate and tropical climates).

Step 2: Obtain the value of k_e (99.9%) from Fig. 2 for the path length in question.

FIGURE 2

Value of k_e exceeded for approximately 99.99% of the worst month (continental temperature climate)

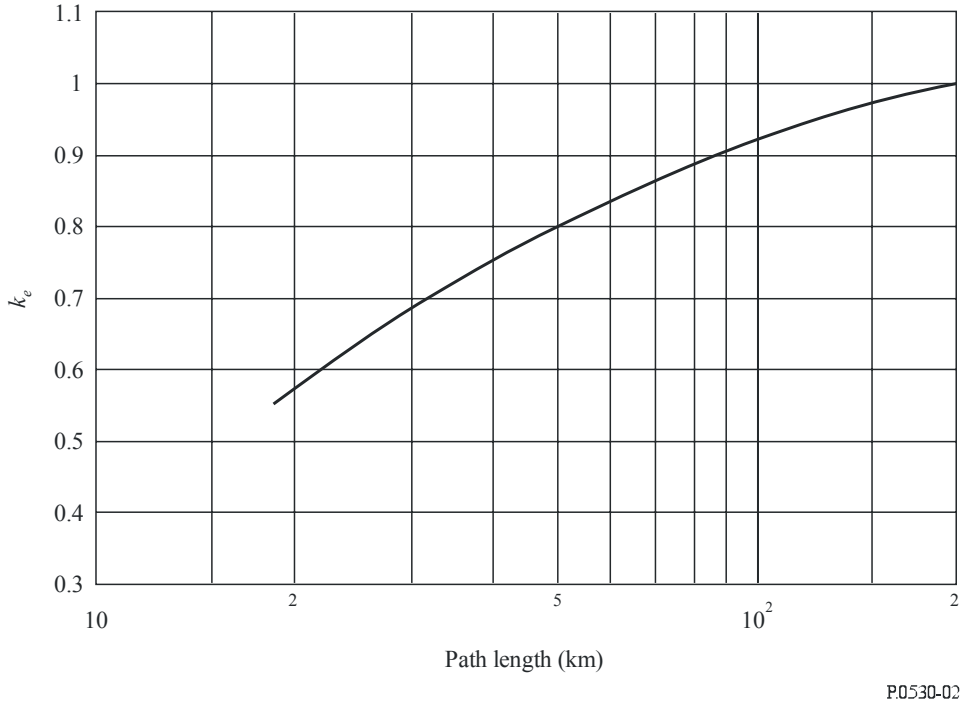

Step 3: Calculate the antenna heights required for the value of k_e obtained from Step 2 and the following Fresnel zone clearance radii:

Temperate climate	Tropical climate
0.0 F1 (i.e. grazing) if there is a single isolated path obstruction 0.3 F1 if the path obstruction is extended along a portion of the path	0.6 F1 for path lengths greater than about 30 km

Step 4: Use the larger of the antenna heights obtained by Steps 1 and 3 (see Note 1).

In cases of uncertainty as to the type of climate, the more conservative clearance rule (see Note 1) for tropical climates may be followed or at least a rule based on an average of the clearances for temperate and tropical climates. Smaller fractions of F_1 may be necessary in Steps 1 and 3 above for frequencies less than about 2 GHz in order to avoid unacceptably large antenna heights.

At frequencies above about 13 GHz, the estimation accuracy of the obstacle height begins to approach the radius of the Fresnel zone. This estimation accuracy should be added to the above clearance.

NOTE 1 – Although these rules are conservative from the viewpoint of diffraction loss due to sub-refractive fading, it must be made clear that an overemphasis on minimizing unavailability due to diffraction loss in sub-refractive conditions may result in a worse degradation of performance and availability in multipath conditions. It is not currently possible to give general criteria for the trade-off to be made between the two conditions. Among the relevant factors are the system fading margins available.

2.2.2.2 Two or three antenna space-diversity configurations

Step 1: Calculate the height of the upper antenna using the procedure for single antenna configurations noted above.

Step 2: Calculate the height of the lower antenna for the appropriate median value of the point k-factor (in the absence of any data use $k = 4/3$) and the following Fresnel zone clearances (see Note 1):

0.6 F_1 to 0.3 F_1 if the path obstruction is extended along a portion of the path;

0.3 F_1 to 0.0 F_1 if there are one or two isolated obstacles on the path profile.

One of the lower values in the two ranges noted above may be chosen if necessary to avoid increasing heights of existing towers or if the frequency is less than 2 GHz.

Alternatively, the clearance of the lower antenna may be chosen to give about 6 dB of diffraction loss during normal refractivity conditions (i.e. during the middle of the day; see § 8), or some other loss appropriate to the fade margin of the system, as determined by test measurements. Measurements should be carried out on several different days to avoid anomalous refractivity conditions.

In this alternative case the diffraction loss can also be estimated using Fig. 1 or equation (2).

Step 3: Verify that the spacing of the two antennas satisfies the requirements for diversity under multipath fading conditions (see § 6.2.1), and if not, modify accordingly.

NOTE 1 – These ranges of clearance were chosen to give a diffraction loss ranging from about 3 dB to 6 dB and to reduce the occurrence of surface multipath fading (see § 6.1.3). Of course, the profiles of some paths will not allow the clearance to be reduced to this range, and other means must be found to ameliorate the effects of multipath fading.

On paths in which surface multipath fading from one or more stable surface reflection is predominant (e.g. overwater or very flat surface areas), it may be desirable to first calculate the height of the upper antenna using the procedure in § 2.2.2.1, and then calculate the minimum optimum spacing for the diversity antenna to protect against surface multipath (see § 6.1.3).

In extreme situations (e.g. very long overwater paths), it may be necessary to employ three-antenna diversity configurations. In this case the clearance of the lowest antenna can be based on the clearance rule in Step 2, and that of the middle antenna on the requirement for optimum spacing with the upper antenna to ameliorate the effects of surface multipath (see § 6.2.1).

2.3 Fading and enhancement due to multipath and related mechanisms

Various clear-air fading mechanisms caused by extremely refractive layers in the atmosphere must be taken into account in the planning of links of more than a few kilometres in length; beam spreading (commonly referred to as defocusing), antenna decoupling, surface multipath, and atmospheric multipath. Most of these mechanisms can occur by themselves or in combination with each other (see Note 1). A particularly severe form of frequency selective fading occurs when beam spreading of the direct signal combines with a surface reflected signal to produce multipath fading. Scintillation fading due to smaller scale turbulent irregularities in the atmosphere is always present with these mechanisms but at frequencies below about 40 GHz its effect on the overall fading distribution is not significant.

NOTE 1 – Antenna decoupling governs the minimum beamwidth of the antennas that should be chosen.

A method for predicting the single-frequency (or narrow-band) fading distribution at large fade depths in the average worst month in any part of the world is given in § 2.3.1. This method does not make use of the path profile and can be used for initial planning, licensing, or design purposes. A second method in § 2.3.2 that is suitable for all fade depths employs the method for large fade depths and an interpolation procedure for small fade depths.

A method for predicting signal enhancement is given in § 2.3.3. The method uses the fade depth predicted by the method in § 2.3.1 as the only input parameter. Finally, a method for converting average worst month to average annual distributions is given in § 2.3.4.

2.3.1 Method for small percentages of time

Step 1: For the path location in question, estimate the geoclimatic factor K for the average worst month from fading data for the geographic area of interest if these are available (see Appendix 1).

If measured data for K are not available, and a detailed link design is being carried out (see Note 1), estimate the geoclimatic factor for the average worst month from:

$$K = 10^{-4.4-0.0027 dN_1} (10 + s_a)^{-0.46} \tag{4}$$

where:

dN_1: point refractivity gradient in the lowest 65 m of the atmosphere not exceeded for 1% of an average year, and s_a is the area terrain roughness

dN_1: provided on a 1.5° grid in latitude and longitude in Recommendation ITU-R P.453. The correct value for the latitude and longitude at path centre should be obtained from the values for the four closest grid points by bilinear interpolation. The data are available in a tabular format and are available from the Radiocommunication Bureau (BR), on the Study Group 3 website

s_a: defined as the standard deviation of terrain heights (m) within a 110 km × 110 km area with a 30 s resolution (e.g. the Globe "gtopo30" data). The area should be aligned with the longitude, such that the two equal halves of the area are on each side of the longitude that goes through the path centre. Terrain data are available from the World Wide Web (the web address is provided by the BR).

If a quick calculation of K is required for planning applications (see Note 1), a fairly accurate estimate can be obtained from:

$$K = 10^{-4.6-0.0027 dN_1} \tag{5}$$

Step 2: From the antenna heights h_e and h_r ((m) above sea level), calculate the magnitude of the path inclination $|\varepsilon_p|$ (mrad) from:

$$|\varepsilon_p| = |h_r - h_e| / d \tag{6}$$

where d is the path length (km).

Step 3: For detailed link design applications (see Notes 1 and 2), calculate the percentage of time p_w that fade depth A (dB) is exceeded in the average worst month from:

$$p_w = Kd^{3.4}(1+|\varepsilon_p|)^{-1.03} f^{0.8} \times 10^{-0.00076h_L - A/10} \quad \% \tag{7}$$

where:

f: frequency (GHz)

h_L: altitude of the lower antenna (i.e. the smaller of h_e and h_r)

and where the geoclimatic factor K is obtained from equation (4).

For quick planning applications as desired (see Notes 1 and 2), calculate the percentage of time p_w that fade depth A (dB) is exceeded in the average worst month from:

$$p_w = Kd^{3.1}(1+|\varepsilon_p|)^{-1.29} f^{0.8} \times 10^{-0.00089h_L - A/10} \quad \% \tag{8}$$

where K is obtained from equation (5).

NOTE 1 – The overall standard deviations of error in predictions using equations (4) and (7), and (5) and (8), are 5.7 dB and 5.9 dB, respectively (including the contribution from year-to-year variability). Within the wide range of paths included in these figures, a minimum standard deviation of error of 5.2 dB applies to overland paths for which $h_L < 700$ m, and a maximum value of 7.3 dB for overwater paths. The small difference between the overall standard deviations, however, does not accurately reflect the improvement in predictions that is available using equations (4) and (7) for links over very rough terrain (e.g. mountains) or very smooth terrain (e.g. overwater paths). Standard deviations of error for mountainous links ($h_L > 700$ m), for example, are reduced by 0.6 dB, and individual errors for links over high mountainous regions by up to several decibels.

NOTE 2 – Equations (7) and (8), and the associated equations (4) and (5) for the geoclimatic factor K, were derived from multiple regressions on fading data for 251 links in various geoclimatic regions of the world with path lengths d in the range of 7.5 to 185 km, frequencies f in the range of 450 MHz to 37 GHz, path inclinations $|\varepsilon_p|$ up to 37 mrad, lower antenna altitudes h_L in the range of 17 to 2 300 m, refractivity gradients dN_1 in the range of –860 to –150 N-unit/km, and area surface roughnesses s_a in the range of 6 to 850 m (for $s_a < 1$ m, use a lower limit of 1 m).

Equations (7) and (8) are also expected to be valid for frequencies to at least 45 GHz. The results of a semi-empirical analysis indicate that the lower frequency limit is inversely proportional to path length. A rough estimate of this lower frequency limit, f_{min}, can be obtained from:

$$f_{min} = 15/d \quad \text{GHz} \tag{9}$$

2.3.2 Method for all percentages of time

The method given below for predicting the percentage of time that any fade depth is exceeded combines the deep fading distribution given in the preceding section and an empirical interpolation procedure for shallow fading down to 0 dB.

Step 1: Using the method in § 2.3.1 calculate the multipath occurrence factor, p_0 (i.e., the intercept of the deep-fading distribution with the percentage of time-axis):

$$p_0 = Kd^{3.4}(1+|\varepsilon_p|)^{-1.03} f^{0.8} \times 10^{-0.00076h_L} \quad \% \tag{10}$$

for detailed link design applications, with K obtained from equation (4), and

$$p_0 = Kd^{3.1}(1+|\varepsilon_p|)^{-1.29} f^{0.8} \times 10^{-0.00089h_L} \quad \% \tag{11}$$

for quick planning applications, with K obtained from equation (5). Note that equations (10) and (11) are equivalent to equations (7) and (8), respectively, with $A = 0$.

Step 2: Calculate the value of fade depth, A_t, at which the transition occurs between the deep-fading distribution and the shallow-fading distribution as predicted by the empirical interpolation procedure:

$$A_t = 25 + 1.2 \log p_0 \quad \text{dB} \tag{12}$$

The procedure now depends on whether A is greater or less than A_t.

Step 3a: If the required fade depth, A, is equal to or greater than A_t:

Calculate the percentage of time that A is exceeded in the average worst month:

$$p_w = p_0 \times 10^{-A/10} \quad \% \tag{13}$$

Note that equation (13) is equivalent to equation (7) or (8), as appropriate.

Step 3b: If the required fade depth, A, is less than A_t:

Calculate the percentage of time, p_t, that A_t is exceeded in the average worst month:

$$p_t = p_0 \times 10^{-A_t/10} \quad \% \tag{14}$$

Note that equation (14) is equivalent to equation (7) or (8), as appropriate, with $A = A_t$.

Calculate q'_a from the transition fade A_t and transition percentage time p_t:

$$q'_a = -20 \log_{10} \left\{ -\ln \left[\left(100 - p_t \right) / 100 \right] \right\} / A_t \tag{15}$$

Calculate q_t from q'_a and the transition fade A_t:

$$q_t = \left(q'_a - 2 \right) \Big/ \left[\left(1 + 0.3 \times 10^{-A_t/20} \right) 10^{-0.016\, A_t} \right] - 4.3 \left(10^{-A_t/20} + A_t/800 \right) \tag{16}$$

Calculate q_a from the required fade A:

$$q_a = 2 + \left[1 + 0.3 \times 10^{-A/20} \right] \left[10^{-0.016\, A} \right] \left[q_t + 4.3 \left(10^{-A/20} + A/800 \right) \right] \tag{17}$$

Calculate the percentage of time, p_w, that the fade depth A (dB) is exceeded in the average worst month:

$$p_w = 100 \left[1 - \exp \left(-10^{-q_a\, A/20} \right) \right] \quad \% \tag{18}$$

Provided that $p_0 < 2\,000$, the above procedure produces a monotonic variation of p_w versus A which can be used to find A for a given value of p_w using simple iteration.

With p_0 as a parameter, Fig. 3 gives a family of curves providing a graphical representation of the method.

FIGURE 3

Percentage of time, p_w, fade depth, A, exceeded in average worst month, with p_0 (in equation (10) or (11), as appropriate) ranging from 0.01 to 1 000

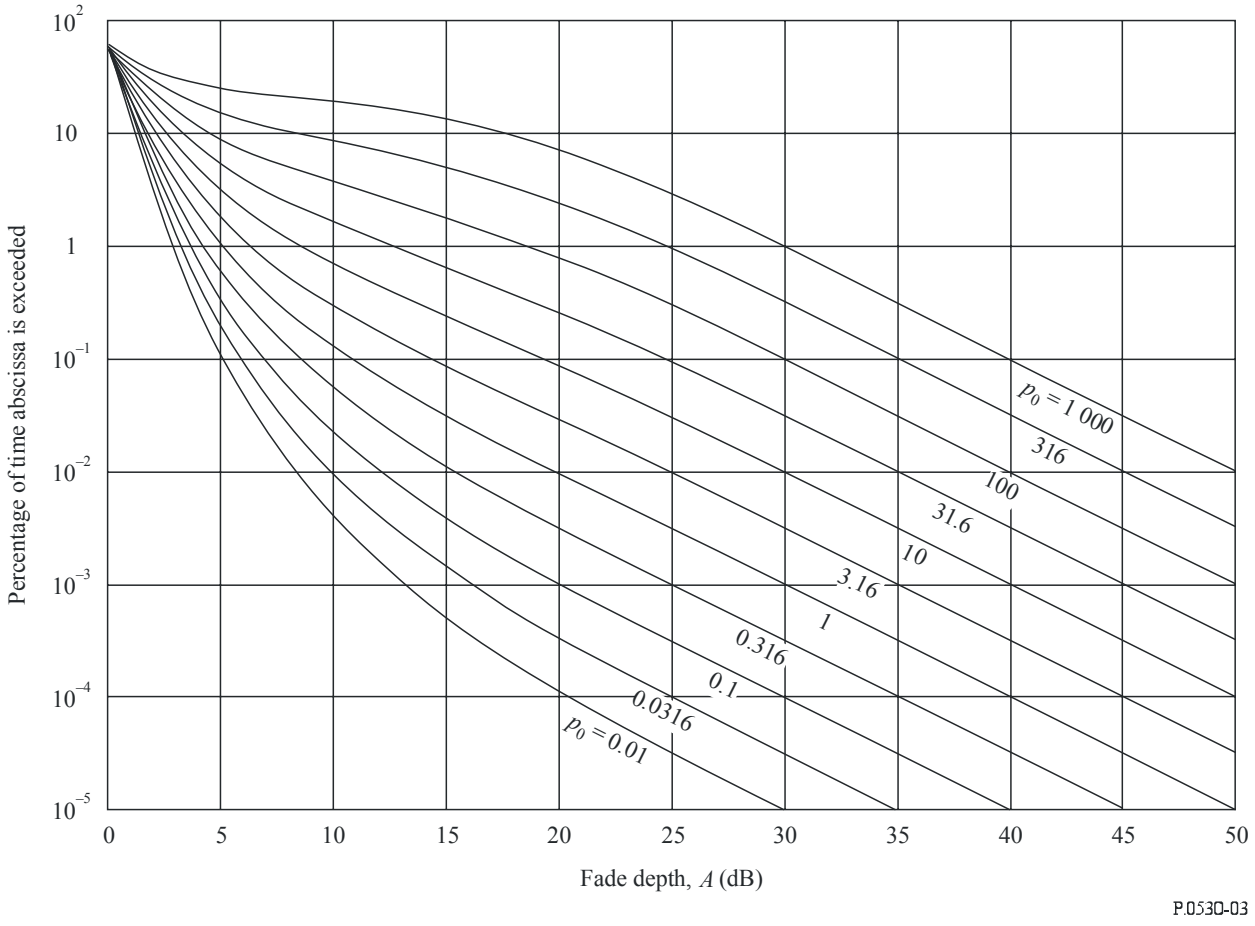

2.3.3 Prediction method for enhancement

Large enhancements are observed during the same general conditions of frequent ducts that result in multipath fading. Average worst month enhancement above 10 dB should be predicted using:

$$p_w = 100 - 10^{(-1.7 + 0.2\,A_{0.01} - E)/3.5} \quad \% \quad \text{for} \quad E > 10 \text{ dB} \tag{19}$$

where E (dB) is the enhancement not exceeded for p% of the time and $A_{0.01}$ is the predicted deep fade depth using equation (7) or (8), as appropriate, exceeded for $p_w = 0.01$% of the time.

For the enhancement between 10 and 0 dB use the following step-by-step procedure:

Step 1: Calculate the percentage of time p'_w with enhancement less or equal to 10 dB ($E' = 10$) using equation (19).

Step 2: Calculate q'_e using:

$$q'_e = -\frac{20}{E'}\left(\log_{10}\left[-\ln\left(1-\frac{100-p'_w}{58.21}\right)\right]\right) \tag{20}$$

Step 3: Calculate the parameter q_s from:

$$q_s = 2.05 q'_e - 20.3 \tag{21}$$

Step 4: Calculate q_e for the desired E using:

$$q_e = 8 + \left[1 + 0.3 \times 10^{-E/20} \right] \left[10^{-0.7E/20} \right] \left[q_s + 12 \left(10^{-E/20} + E/800 \right) \right] \tag{22}$$

Step 5: The percentage of time that the enhancement E (dB) is not exceeded is found from:

$$p_w = 100 - 58.21 \left[1 - \exp\left(-10^{-q_e E/20} \right) \right] \tag{23}$$

The set of curves in Fig. 4 gives a graphical representation of the method with p_0 as parameter (see equation (10) or (11), as appropriate). Each curve in Fig. 4 corresponds to the curve in Fig. 3 with the same value of p_0. It should be noted that Fig. 4 gives the percentage of time for which the enhancements are exceeded which corresponds to $(100 - p_w)$, with p_w given by equations (19) and (23).

FIGURE 4

Percentage of time, $(100 - p_w)$, enhancement, E, exceeded in the average worst month, with p_0 (in equation (10) or (11), as appropriate) ranging from 0.01 to 1 000

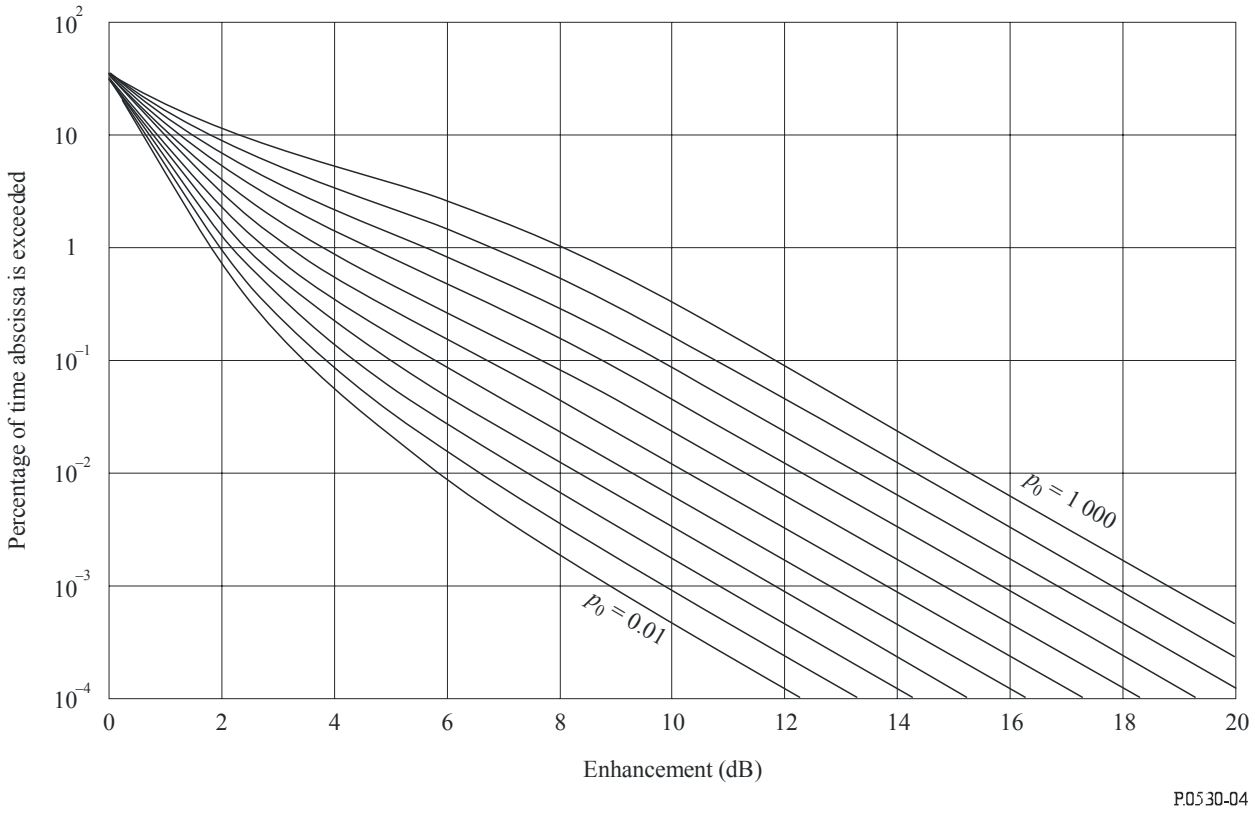

For prediction of exceedance percentages for the average year instead of the average worst month, see § 2.3.4.

2.3.4 Conversion from average worst month to average annual distributions

The fading and enhancement distributions for the average worst month obtained from the methods of § 2.3.1 to 2.3.3 can be converted to distributions for the average year by employing the following procedure:

Step 1: Calculate the percentage of time p_w fade depth A is exceeded in the large tail of the distribution for the average worst month from equation (7) or (8), as appropriate.

Step 2: Calculate the logarithmic geoclimatic conversion factor ΔG from:

$$\Delta G = 10.5 - 5.6 \log\left(1.1 \pm |\cos 2\xi|^{0.7}\right) - 2.7 \log d + 1.7 \log\left(1 + |\varepsilon_p|\right) \quad \text{dB} \qquad (24)$$

where $\Delta G \leq 10.8$ dB and the positive sign is employed for $\xi \leq 45°$ and the negative sign for $\xi > 45°$ and where:

ξ: latitude (°N or °S)

d: path length (km)

$|\varepsilon_p|$: magnitude of path inclination (obtained from equation (6)).

Step 3: Calculate the percentage of time p fade depth A is exceeded in the large fade depth tail of the distribution for the average year from:

$$p = 10^{-\Delta G / 10} p_w \quad \% \qquad (25)$$

Step 4: If the shallow fading range of the distribution is required, follow the method of Step 3b of § 2.3.2, with the following changes:

1) Convert the value of p_t obtained in equation (14) to an annual value by using equation (25), and use this annual value instead of p_t where p_t appears in equation (15).

2) The value of p_w calculated by equation (18) is the required annual value p.

Step 5: If it is required to predict the distribution of enhancement for the average year, follow the method of § 2.3.3, where $A_{0.01}$ is now the fade depth exceeded for 0.01% of the time in the average year. Obtain first p_w by inverting equation (25) and using p = 0.01%. Then obtain fade depth $A_{0.01}$ exceeded for 0.01% of the time in the average year by inverting equation (7) or (8), as appropriate, and using p in place of p_w.

2.3.5 Conversion from average worst month to shorter worst periods of time

The percentage of time p_w of exceeding a deep fade A in the average worst month can be converted to a percentage of time p_{sw} of exceeding the same deep fade during a shorter worst period of time T by the relations:

$$p_{sw} = p_w \cdot \left(89.34 T^{-0.854} + 0.676\right) \quad \% \quad 1 \text{ h} \leq T < 720 \text{ h for relatively flat paths} \qquad (26)$$

$$p_{sw} = p_w \cdot \left(119 T^{-0.78} + 0.295\right) \quad \% \quad 1 \text{ h} \leq T < 720 \text{ h for hilly paths} \qquad (27)$$

$$p_{sw} = p_w \cdot \left(199.85 T^{-0.834} + 0.175\right) \quad \% \quad 1 \text{ h} \leq T < 720 \text{ h for hilly land paths} \qquad (28)$$

NOTE 1 – Equations (26) to (28) were derived from data for 25 links in temperate regions for which p_w was estimated from data for summer months.

2.3.6 Prediction of non-selective outage (see Note 1)

In the design of a digital link, calculate the probability of outage P_{ns} due to the non-selective component of the fading (see § 7) from:

$$P_{ns} = p_w / 100 \tag{29}$$

where p_w(%) is the percentage of time that the flat fade margin $A = F$ (dB) corresponding to the specified bit error ratio (BER) is exceeded in the average worst month (obtained from § 2.3.1 or § 2.3.2, as appropriate). The flat fade margin, F, is obtained from the link calculation and the information supplied with the particular equipment, also taking into account possible reductions due to interference in the actual link design.

NOTE 1 – For convenience, the outage is here defined as the probability that the BER is larger than a given threshold, whatever the threshold (see § 7 for further information).

2.3.7 Occurrence of simultaneous fading on multi-hop links

Experimental evidence indicates that, in clear-air conditions, deep fades on adjacent hops in a multi-hop link are almost completely uncorrelated. This applies whether frequency selective fading, flat fading or a combination occurs.

For a multi-hop link, an upper bound to the total outage probability for clear-air effects can be obtained by summing the outage probabilities of the individual hops. A closer upper bound to the probability of exceeding a fade depth A (dB) on the link of n hops can be estimated from (see Note 1):

$$P_T = \sum_{i=1}^{n} P_i - \sum_{i=1}^{n-1} (P_i P_{i+1})^C \tag{30}$$

$$C = 0.5 + 0.0052A + 0.0025(d_A + d_B) \tag{31}$$

where P_i is the outage probability predicted for the i-th of the total n hops and d_i the path length (km) of the i-th hop. Equation (31) should be used for $A \leq 40$ dB and $(d_i + d_{i+1}) \leq 120$ km. Above these limits, $C = 1$.

NOTE 1 – Equation (31) was derived based on the results of measurements on 19 pairs of adjacent line-of-sight hops operating in the 4 and 6 GHz bands, with path lengths in the range of 33 to 64 km.

2.4 Attenuation due to hydrometeors

Attenuation can also occur as a result of absorption and scattering by such hydrometeors as rain, snow, hail and fog. Although rain attenuation can be ignored at frequencies below about 5 GHz, it must be included in design calculations at higher frequencies, where its importance increases rapidly. A technique for estimating long-term statistics of rain attenuation is given in § 2.4.1. On paths at high latitudes or high altitude paths at lower latitudes, wet snow can cause significant attenuation over an even larger range of frequencies. More detailed information on attenuation due to hydrometeors other than rain is given in Recommendation ITU-R P.840.

At frequencies where both rain attenuation and multipath fading must be taken into account, the exceedance percentages for a given fade depth corresponding to each of these mechanisms can be added.

2.4.1 Long-term statistics of rain attenuation

The following simple technique may be used for estimating the long-term statistics of rain attenuation:

Step 1: Obtain the rain rate $R_{0.01}$ exceeded for 0.01% of the time (with an integration time of 1 min). If this information is not available from local sources of long-term measurements, an estimate can be obtained from the information given in Recommendation ITU-R P.837.

Step 2: Compute the specific attenuation, γ_R (dB/km) for the frequency, polarization and rain rate of interest using Recommendation ITU-R P.838.

Step 3: Compute the effective path length, d_{eff}, of the link by multiplying the actual path length d by a distance factor r. An estimate of this factor is given by:

$$r = \frac{1}{0.477\ d^{0.633}\ R_{0.01}^{0.073 \cdot \alpha}\ f^{0.123} - 10.579\ (1 - \exp(-0.024\ d))} \tag{32}$$

where f (GHz) is the frequency and α is the exponent in the specific attenuation model from Step 2. Maximum recommended r is 2.5, such that equation (32) is not used for small values of the denominator giving larger values.:

Step 4: An estimate of the path attenuation exceeded for 0.01% of the time is given by:

$$A_{0.01} = \gamma_R\ d_{eff} = \gamma_R\ dr \qquad \text{dB} \tag{33}$$

Step 5: The attenuation exceeded for other percentages of time p in the range 0.001% to 1% may be deduced from the following power law:

$$\frac{A_p}{A_{0.01}} = C_1\ p^{-(C_2 + C_3 \log_{10} p)} \tag{34}$$

with:

$$C_1 = \left(0.07^{C_0}\right)\left[0.12^{(1-C_0)}\right] \tag{35a}$$

$$C_2 = 0.855 C_0 + 0.546\left(1 - C_0\right) \tag{35b}$$

$$C_3 = 0.139 C_0 + 0.043\left(1 - C_0\right) \tag{35c}$$

where:

$$C_0 = \begin{cases} 0.12 + 0.4\left[\log_{10}\left(f/10\right)^{0.8}\right] & f \geq 10\ GHz \\ 0.12 & f < 10\ GHz \end{cases} \tag{36}$$

Step 6: If worst-month statistics are desired, calculate the annual time percentages p corresponding to the worst-month time percentages p_w using climate information specified in Recommendation ITU-R P.841. The values of A exceeded for percentages of the time p on an annual basis will be exceeded for the corresponding percentages of time p_w on a worst-month basis.

The prediction procedure outlined above is considered to be valid in all parts of the world at least for frequencies up to 100 GHz and path lengths up to 60 km.

2.4.2 Combined method for rain and wet snow

The attenuation, A_p, exceeded for time percentage p given by the previous sub-section is valid for link paths through which only liquid rain falls.

For high latitudes or high link altitudes, higher values of attenuation may be exceeded for time percentage p due to the effect of melting ice particles or wet snow in the melting layer. The incidence of this effect is determined by the height of the link in relation to the rain height, which varies with geographic location. The variation of zero-degree rain height is taken into account in the following method by taking 49 height values relative to the median of the rain height, with a probability associated with each given by Table 1.

The following method is not needed if it is known that a link is never affected by the melting layer. If this is not known, the calculation for rain given above should be used to calculate A_p, and then the following steps should be followed:

Step 1: Obtain the median rain height, h_{rainm}, metres above mean sea level (amsl) from Recommendation ITU-R P.839.

Step 2: Calculate the rain height of the centre of the link path, h_{link}, taking median-Earth curvature into account using:

$$h_{link} = 0.5(h_1 + h_2) - (D^2/17) \quad \text{m amsl} \tag{37}$$

where:

$h_{1,2}$: height of the link terminals (amsl)

D: path length (km).

Step 3: A test may now be made to determine whether there is a possibility of additional attenuation. If $h_{link} \leq h_{rainm} - 3\,600$, the link will not be affected by melting-layer conditions and A_p can be taken as the attenuation exceeded for p% of the time, and this method can be stopped. Otherwise, the method continues with the following steps.

Step 4: Initialize a multiplying factor, F, to zero.

Step 5: For successive values of the index i = 0, 1, 2, to 48, in order:

a) Calculate the rain height, h_{rain}, using:

$$h_{rain} = h_{rainm} - 2400 + 100i \quad \text{m amsl} \tag{38}$$

b) Calculate the link height relative to the rain height using:

$$\Delta h = h_{link} - h_{rain} \quad \text{m} \tag{39}$$

c) Calculate the addition to the multiplying factor for this value of the index i:

$$\Delta F = \Gamma(\Delta h) P_i \tag{40}$$

where:

$\Gamma(\Delta h)$ is a multiplying factor which takes account of differing specific attenuations according to height relative to the rain height, given by:

$$\Gamma(\Delta h) = \begin{cases} 0 & 0 < \Delta h \\ \dfrac{4\left(1 - e^{\Delta h/70}\right)^2}{\left(1 + \left(1 - e^{-(\Delta h/600)^2}\right)^2 \left(4\left(1 - e^{\Delta h/70}\right)^2 - 1\right)\right)} & -1200 \le \Delta h \le 0 \\ 1 & \Delta h < -1200 \end{cases} \quad (41)$$

and P_i is the probability that the link will be at Δh, taken from Table 1.

d) Add ΔF to the current value of F. This operation may be represented as a procedure by the expression:

$$F = F + \Delta F \quad \text{dB} \quad (42)$$

Step 6: Calculate the combined rain and wet snow attenuation using:

$$A_{rs} = A_p \cdot F \quad (43)$$

Depending on the height of the link relative to the median rain height, A_{rs} can be more than or less than A_p. Near the poles of the Earth it is possible for the link to be always above the rain height, in which case A_{rs} is zero.

TABLE 1

Index "*i*"		**Probability P_i**
Either	**Or**	
0	48	0.000555
1	47	0.000802
2	46	0.001139
3	45	0.001594
4	44	0.002196
5	43	0.002978
6	42	0.003976
7	41	0.005227
8	40	0.006764
9	39	0.008617
10	38	0.010808
11	37	0.013346
12	36	0.016225
13	35	0.019419
14	34	0.022881
15	33	0.026542
16	32	0.030312

TABLE 1 (*end*)

Index "*i*"		Probability P_i
Either	**Or**	
17	31	0.034081
18	30	0.037724
19	29	0.041110
20	28	0.044104
21	27	0.046583
22	26	0.048439
23	25	0.049588
24		0.049977

2.4.3 Frequency scaling of long-term statistics of rain attenuation

When reliable long-term attenuation statistics are available at one frequency the following empirical expression may be used to obtain a rough estimate of the attenuation statistics for other frequencies in the range 7 to 50 GHz, for the same hop length and in the same climatic region:

$$A_2 = A_1 \, (\Phi_2 / \Phi_1)^{1 - H(\Phi_1, \Phi_2, A_1)} \tag{44}$$

where:

$$\Phi(f) = \frac{f^2}{1 + 10^{-4} \, f^2} \tag{45}$$

$$H(\Phi_1, \Phi_2, A_1) = 1.12 \times 10^{-3} \, (\Phi_2 / \Phi_1)^{0.5} \, (\Phi_1 \, A_1)^{0.55} \tag{46}$$

Here, A_1 and A_2 are the equiprobable values of the excess rain attenuation at frequencies f_1 and f_2 (GHz), respectively.

2.4.4 Polarization scaling of long-term statistics of rain attenuation

Where long-term attenuation statistics exist at one polarization (either vertical (V) or horizontal (H)) on a given link, the attenuation for the other polarization over the same link may be estimated through the following simple formulae:

$$A_V = \frac{300 \, A_H}{335 + A_H} \quad \text{dB} \tag{47}$$

or

$$A_H = \frac{335 \, A_V}{300 - A_V} \quad \text{dB} \tag{48}$$

These expressions are considered to be valid in the range of path length and frequency for the prediction method of § 2.4.1.

2.4.5 Statistics of event duration and number of events

Although there is little information as yet on the overall distribution of fade duration, there are some data and an empirical model for specific statistics such as mean duration of a fade event and the number of such events. An observed difference between the average and median values of duration indicates, however, a skewness of the overall distribution of duration. Also, there is strong evidence that the duration of fading events in rain conditions is much longer than those during multipath conditions.

An attenuation event is here defined to be the exceedance of attenuation A for a certain period of time (e.g., 10 s or longer). The relationship between the number of attenuation events $N(A)$, the mean duration $D_m(A)$ of such events, and the total time $T(A)$ for which attenuation A is exceeded longer than a certain duration, is given by:

$$N(A) = T(A) / D_m(A) \tag{49}$$

The total time $T(A)$ depends on the definition of the event. The event usually of interest for application is one of attenuation A lasting for 10 s or longer. However, events of shorter duration (e.g., a sampling interval of 1 s used in an experiment) are also of interest for determining the percentage of the overall outage time attributed to unavailability (i.e., the total event time lasting 10 s or longer).

The number of fade events exceeding attenuation A for 10 s or longer can be represented by (see Note 1):

$$N_{10s}(A) = 1 + 1313 \cdot [p(A)]^{0.945} \tag{50}$$

where $p(A)$ is the percentage of time that the rain attenuation A(dB) exceeded in the average year. If this information is not available from local sources of long-term measurements, it can be obtained by numerically solving equation (34) in § 2.4.1.

NOTE 1 − Equation (50) is based on the results of measurements during 1 to 3 years on 27 links, with frequencies in the range from 12.3 to 83 GHz and path lengths in the range of 1.2 to 43 km, in Brazil, Norway, Japan and Russia.

The outage intensity (OI) is defined as the number of unavailability events per year. For a digital radio link, an unavailability event occurs whenever a specified bit error rate is exceeded for periods over 10 seconds. The following method should be used for the prediction of outage intensity due to rain attenuation on single-hop links:

Step 1: Obtain the percentage of time $p(M)$ that the link margin M(dB) for rain attenuation is exceeded. If this information is not available from local sources of long-term measurements, it can be obtained by numerically solving equation (34) in § 2.4.1 with $A_p = M$.

Step 2: An estimate of the outage intensity due to rain is given by:

$$OI(M) = N_{10s}(M) \tag{51}$$

where M(dB) is the link margin associated to the bit error rate or block error rate of interest and N_{10s} is given by equation (50).

Based on a set of measurements (from an 18 GHz, 15 km path on the Scandinavian peninsula), 95-100% of all rain events greater than about 15 dB can be attributed to unavailability. With such a fraction known, the unavailability can be obtained by multiplying this fraction by the total percentage of time that a given attenuation A is exceeded as obtained from the method of § 2.4.1.

2.4.6 Rain attenuation in multiple hop networks

There are several configurations of multiple hops of interest in point-to-point networks in which the non-uniform structure of hydrometeors plays a role. These include a series of hops in a tandem network and more than one such series of hops in a route-diversity network.

2.4.6.1 Length of individual hops in a tandem network

The overall transmission performance of a tandem network is largely influenced by the propagation characteristics of the individual hops. It is sometimes possible to achieve the same overall physical connection by different combinations of hop lengths. Increasing the length of individual hops inevitably results in an increase in the probability of outage for those hops. On the other hand, such a move could mean that fewer hops might be required and the overall performance of the tandem network might not be impaired.

2.4.6.2 Correlated fading on tandem hops

If the occurrence of rainfall were statistically independent of location, then the overall probability of fading for a linear series of links in tandem would be given to a good approximation by:

$$P_T = \sum_{i=1}^{n} P_i \tag{52}$$

where P_i is the probability of fading for the i-th of the total n links.

On the other hand, if precipitation events are correlated over a finite area, then the attenuation on two or more links of a multi-hop relay system will also be correlated, in which case the combined fading probability may be written as:

$$P_T = K \sum_{i=1}^{n} P_i \tag{53}$$

where K is a modification factor that includes the overall effect of rainfall correlation.

Few studies have been conducted with regard to this question. One such study examined the instantaneous correlation of rainfall at locations along an East-West route, roughly parallel to the prevailing direction of storm movement. Another monitored attenuation on a series of short hops oriented North-South, or roughly perpendicular to the prevailing storm track during the season of maximum rainfall.

For the case of links parallel to the direction of storm motion, the effects of correlation for a series of hops each more than 40 km in length, l, were slight. The modification factor, K, in this case exceeded 0.9 for rain induced outage of 0.03% and may reasonably be ignored (see Fig. 5). For shorter hops, however, the effects become more significant: the overall outage probability for 10 links of 20, 10 and 5 km each is approximately 80%, 65% and 40% of the uncorrelated expectation, respectively (modification factors 0.8, 0.65, 0.4). The influence of rainfall correlation is seen to be somewhat greater for the first few hops and then decreases as the overall length of the chain increases.

The modification factors for the case of propagation in a direction perpendicular to the prevailing direction of storm motion are shown in Fig. 6 for several probability levels. In this situation, the modification factors fall more rapidly for the first few hops (indicating a stronger short-range

correlation than for propagation parallel to storm motion) and maintain relatively steady values thereafter (indicating a weaker long-range correlation).

2.4.6.3 Route-diversity networks

Making use of the fact that the horizontal structure of precipitation can change significantly within the space of a fraction of a kilometre, route diversity networks can involve two or more hops in tandem in two or more diversity routes. Although there is no information on diversity improvement for complete route diversity networks, there is some small amount of information on elements of such a network. Such elements include two paths converging at a network node, and approximately parallel paths separated horizontally.

FIGURE 5

Modification factor for joint rain attenuation on a series of tandem hops of equal length, *l*, for an exceedance probability of 0.03% for each link

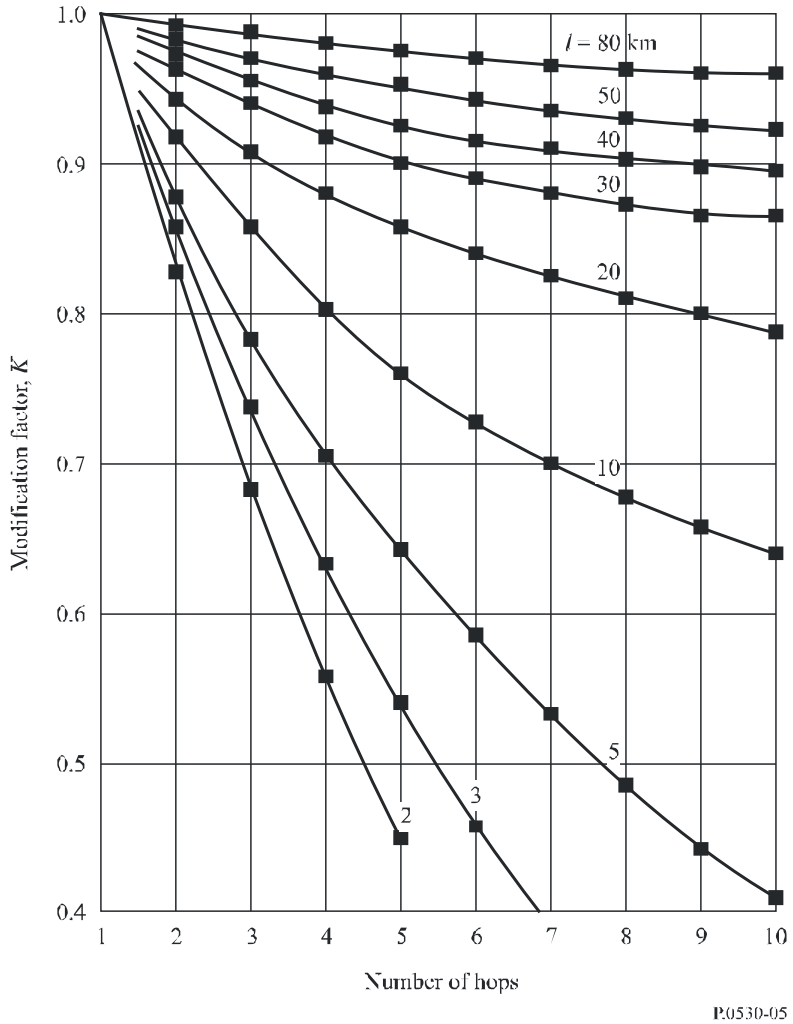

2.4.6.3.1 Convergent path elements

Information on the diversity improvement factor for converging paths in the low EHF range of the spectrum can be found in Recommendation ITU-R P.1410. Although developed for point-to-area applications, it can be used to give some general indication of the improvement afforded by such elements of a point-to-point route-diversity (or mesh) network, of which there would be two.

Due to the random temporal and spatial distribution of the rainfall rate, convergent point-to-point links will instantaneously experience different depths of attenuation. As a result, there may be a degradation in the *S*/*I* between links from users in different angular sectors whenever the desired signal is attenuated by rain in its path and the interfering signal is not.

The differential rain attenuation (DRA) cumulative distribution for two convergent links operating at the same frequency can be estimated by employing the following steps:

Step 1: Approximate the annual distribution of rain attenuation A_i (in dB) over each path i=1,2 by employing the log-normal distribution:

$$P(A_i)=\frac{1}{2}\text{erfc}\left(\frac{\ln A_i-\ln A_{mi}}{\sqrt{2}S_{ai}}\right) \tag{54}$$

where $\text{erfc}(x)= 2/\sqrt{\pi}\int_x^\infty e^{-t^2}\,dt$ is the complementary error function. To calculate A_{mi} and S_{ai}, a fitting procedure over either available local measurements or the rain attenuation distribution in § 2.4.1 of Recommendation ITU-R P.530-12 is recommended. This procedure is detailed in Annex 2 of Recommendation ITU-R P.1057-2.

Step 2: Determine the rain inhomogeneity constant D_r, that is the distance in km the correlation coefficient becomes equal to $\sqrt{2}/2$. A simple rule for calculating D_r depends on the absolute latitude $|lat|$ of the location:

$$D_r=\begin{cases}1 & |lat|\le 23^\circ\\ 1.5 & 23^\circ<|lat|\le 50^\circ\\ 1.75 & |lat|>50^\circ\end{cases} \tag{55}$$

Step 3: Determine the characteristic distance of the rainfall area as $D_c = 20 \times D_r$.

Step 4: Evaluate the spatial parameter H_i, i=1,2, over each of the alternative path of length L_i:

$$H_i = 2L_iD_r\sinh^{-1}\left(L_i/D_r\right)+2D_r^{\,2}\left(1-\sqrt{\left(L_i/D_r\right)^2+1}\right),\quad i=1,2 \tag{56}$$

Step 5: Evaluate the spatial parameter H_{12} between the two paths:

$$H_{12}=\int_0^{L_1}\int_0^{L_2}\rho_0(d)\,d\ell_1\,d\ell_2 \tag{57}$$

where:

$$\rho_0(d)=\begin{cases}\dfrac{D_r}{\sqrt{D_r^{\,2}+d^2}} & d\le D_c\\[2ex] \dfrac{D_r}{\sqrt{D_r^{\,2}+D_c^2}} & d>D_c\end{cases} \tag{58}$$

and the distance of two points of the alternative paths forming an angle φ is given by:

$$d^2=\ell_1^2+\ell_2^2-2\ell_1\ell_2\cos\phi,\qquad 0<\ell_1\le L_1,\ 0<\ell_2\le L_2 \tag{59}$$

Step 6: Calculate the correlation coefficient of rain attenuation:

$$\rho_a = \frac{1}{S_{a1} S_{a2}} = \ln\left[\frac{H_{12}}{\sqrt{H_1 H_2}} \left(e^{S_{a1}^2} - 1 \right)^{1/2} \left(e^{S_{a2}^2} - 1 \right)^{1/2} + 1 \right] \tag{60}$$

Step 7: The cumulative distribution of DRA A_1-A_2 exceeding the threshold δA (in dB) is given by:

$$P_{DRA} = \frac{1}{2} \operatorname{erfc}\left(\frac{u_{01}}{\sqrt{2}} \right) - \frac{1}{2} \int_{u_{01}}^{\infty} \frac{1}{\sqrt{2\pi}} \exp\left(-\frac{u_1^2}{2} \right) \operatorname{erfc}\left(\frac{u_{02} - \rho_a u_1}{\sqrt{2}\sqrt{1-\rho_a^2}} \right) du_1 \tag{61}$$

where:

$$u_i = \frac{\ln A_i - \ln A_{mi}}{S_{ai}}, \qquad i = 1, 2 \tag{62}$$

$$u_{01} = \frac{\ln \delta a - \ln A_{m1}}{S_{a1}} \tag{63}$$

$$u_{02} = \frac{\ln\left(A_{m1} \exp(u_1 S_{a1}) - \delta a \right) - \ln A_{m2}}{S_{a2}} \tag{64}$$

2.4.6.3.2 Parallel paths separated horizontally

Experimental data obtained in the United Kingdom in the 20-40 GHz range give an indication of the improvement in link reliability which can be obtained by the use of parallel-path elements of route-diversity networks, as shown in Fig. 6a. The diversity gain (i.e. the difference between the attenuation (dB) exceeded for a specific percentage of time on a single link and that simultaneously on two parallel links):

– tends to decrease as the path length increases from 12 km for a given percentage of time, and for a given lateral path separation;

– is generally greater for a spacing of 8 km than for 4 km, though an increase to 12 km does not provide further improvement;

– is not significantly dependent on frequency in the range 20-40 GHz, for a given geometry; and

– ranges from about 2.8 dB at 0.1% of the time to 4.0 dB at 0.001% of the time, for a spacing of 8 km, and path lengths of about the same value. Values for a 4 km spacing are about 1.8 to 2.0 dB.

The necessary steps for deriving the diversity improvement I and the diversity gain G for completely parallel paths are the following:

FIGURE 6

(a) Parallel route diversity geometry.
(b) Route diversity geometry that deviates from being completely parallel.

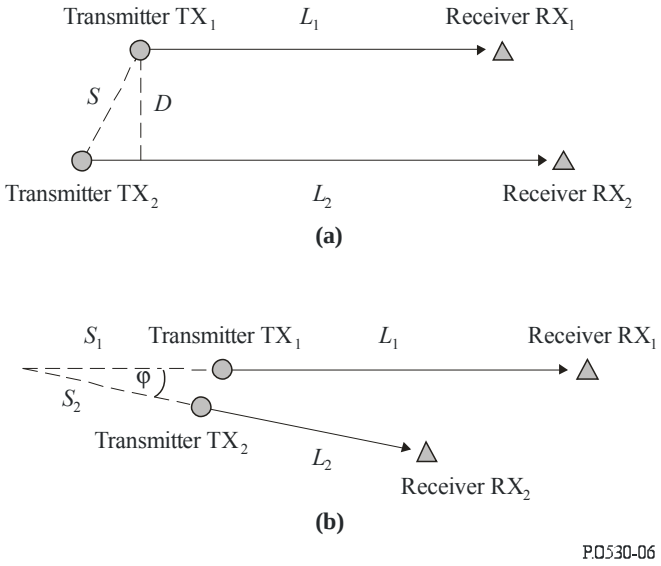

Step 1: Follow Steps 1 to 4 of § 2.4.6.3.1.

Step 2: Calculate H_{12} according to (57). Due to the change of geometry from converging to parallel paths, there is a modification in Step 5 of the procedure outlined in § 2.4.6.3.1. Specifically, the definition of the distance d between two points of the alternative path elements, which is used for the calculation of the correlation coefficient $\rho_0(d)$ in (58) is, in this case, expressed as:

$$d^2 = S^2 + 2\sqrt{S^2 - D^2}\,|\ell_1 - \ell_2| + (\ell_1 - \ell_2)^2 \qquad 0 < \ell_1 \le L_1,\ \ 0 < \ell_2 \le L_2 \tag{65}$$

where the parallel paths are separated horizontally by a distance D and S is the distance between the two transmitters (see Fig. 6a).

Step 3: Repeat Step 6 of § 2.4.6.3.1 employing the value of H_{12} derived in Step 2.

Step 4: The cumulative distribution of the parallel diversity configuration exceeding a fade depth A_i is given by:

$$P_d(A_i) = \frac{1}{2}\int_{u_2}^{\infty} \frac{1}{\sqrt{2\pi}} \exp\left(-\frac{u^2}{2}\right) \operatorname{erfc}\left(\frac{u_1 - \rho_a u}{\sqrt{2}\sqrt{1-\rho_a}}\right) du \tag{66}$$

where u_i, i=1,2, is given in (62).

Step 5: The diversity improvement I at the reference attenuation level A_i is obtained based on the relationship:

$$I(A_i) = \frac{P(A_i)}{P_d(A_i)}, \qquad i=1,2 \tag{67}$$

Step 6: The diversity gain G at the reference percentage t is obtained based on the relationship (see Note 1):

$$G(A_i) = A_i(t) - A_d(t), \qquad i=1,2 \tag{68}$$

NOTE 1 – To calculate $A_i(t)$ and $A_d(t)$ in equation (68), equations (54) and (66) must be reversed.

For reversing equation (66), a numerical analysis must be applied.

In case the two alternative paths deviate significantly from being completely parallel to one another, as shown in Fig. 6b, the extensions of the two links intersect at a certain point at distances S_1 and S_2 from the two transmitters. Again, to produce the diversity figure of merits (gain and improvement), Steps 1 through 6 of the current section are repeated. However, in this case, d is given by (59) and H_{12} is written as:

$$H_{12} = \int_{S_1}^{S_1+L_1} \int_{S_2}^{S_2+L_2} \rho_0 \left(d = \left|\ell_1 - \ell_2\right|\right) d\ell_1 d\ell_2 \tag{69}$$

FIGURE 7

Modification factor for joint rain attenuation on a series of tandem hops of approximately 4.6 km each for several exceedance probability levels for each link

(May 1975-March 1979)

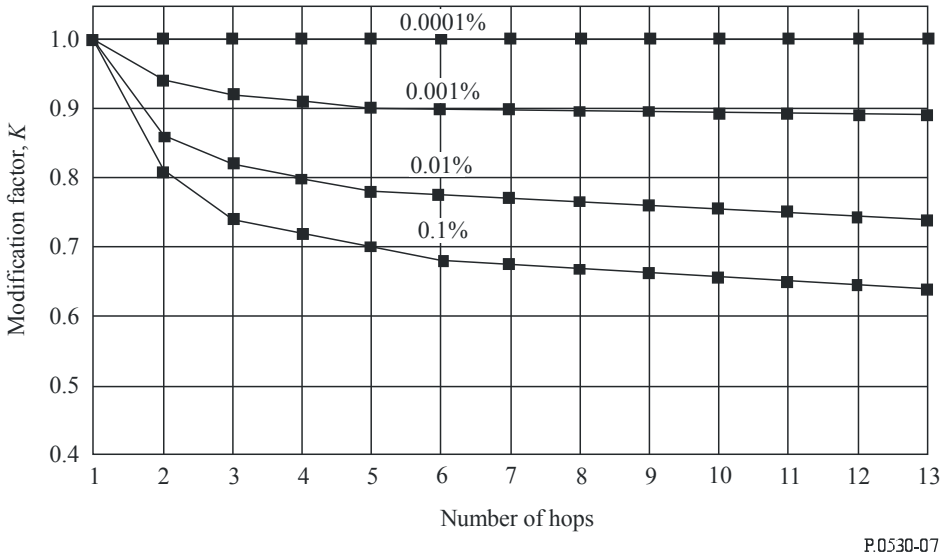

2.4.6.4 Paths with passive repeaters

2.4.6.4.1 Plane-reflector repeaters

For paths with two or more legs (N in total) for which plane passive reflectors are used and for which the legs are within a few degrees of being parallel (see Note 1), calculate the rain attenuation on the overall path by substituting the path length.

$$d = d_{leg1} + d_{leg2} + \ldots + d_{legN} \quad \text{km} \tag{70}$$

into the method of § 2.4.1, including into the calculation of the distance reduction factor from equation (32).

NOTE 1 – No strict guideline can be given at the present time on how closely the legs should be parallel. If the legs are not parallel, the approach in equation (70) will result in a reduction factor r in equation (32) that is smaller than it should be, thus causing the actual total attenuation to be underestimated. A possible solution to this might be to employ both equation (70) and the path length obtained by joining the ends of first and last leg in the calculation of the reduction factor alone, and averaging the results.

An alternative approach might be to treat the legs as independent paths and apply the information in § 2.4.6.

2.4.6.4.2 Back-to-back-antenna repeaters

If the two or more legs of the path use the same polarization, calculate the attenuation statistics using the method of § 2.4.6.4.1 for plane reflectors.

If the legs of the path use different polarizations, apply the method of § 2.4.1 along with equation (70) for both horizontal and vertical polarization to obtain the percentages of time p_H and p_V for which the desired attenuation is exceeded (see Note 1) with horizontal and vertical polarization, respectively. Use equation (70) to calculate the total path length d_H for those legs using horizontal polarization and also to calculate the total path length d_V for those legs using vertical polarization. Then calculate the percentage of time p that the given attenuation is exceeded on the overall path from (see Note 2):

$$p = \frac{p_H d_H + p_V d_V}{d_H + d_V} \quad \% \tag{71}$$

NOTE 1 – Since the method of § 2.4.1 provides the attenuation exceeded for a given percentage of time, it must be inverted numerically to obtain the percentage of time that a given attenuation is exceeded.

NOTE 2 – If the legs of the path deviate significantly from being parallel to one another, it is likely that an approach similar to that suggested in Note 1 of § 2.4.6.4.1 might be employed to improve accuracy. In this case, it would have to be employed to calculate the attenuation for each polarization separately.

2.4.7 Prediction of outage due to precipitation

In the design of a digital link, calculate the probability, P_{rain}, of exceeding a rain attenuation equal to the flat fade margin F (dB) (see § 2.3.5) for the specified BER from:

$$P_{rain} = p/100 \tag{72}$$

where p (%) is the percentage of time that a rain attenuation of F (dB) is exceeded in the average year by solving equation (34) in § 2.4.1.

3 Variation in angle-of-arrival/launch

Abnormal gradients of the clear-air refractive index along a path can cause considerable variation in the angles of launch and arrival of the transmitted and received waves. This variation is substantially frequency independent and primarily in the vertical plane of the antennas. The range of angles is greater in humid coastal regions than in dry inland areas. No significant variations have been observed during precipitation conditions.

The effect can be important on long paths in which high gain/narrow beam antennas are employed. If the antenna beamwidths are too narrow, the direct outgoing/incoming wave can be sufficiently far off axis that a significant fade can occur (see § 2.3). Furthermore, if antennas are aligned during periods of very abnormal angles-of-arrival, the alignment may not be optimum. Thus, in aligning antennas on critical paths (e.g. long paths in coastal area), it may be desirable to check the alignment several times over a period of a few days.

4 Reduction of cross-polar discrimination (XPD)

The XPD can deteriorate sufficiently to cause co-channel interference and, to a lesser extent, adjacent channel interference. The reduction in XPD that occurs during both clear-air and precipitation conditions must be taken into account.

4.1 Prediction of XPD outage due to clear-air effects

The combined effect of multipath propagation and the cross-polarization patterns of the antennas governs the reductions in XPD occurring for small percentages of time. To compute the effect of these reductions in link performance the following step-by-step procedures should be used:

Step 1: Compute:

$$XPD_0 = \begin{cases} XPD_g + 5 & \text{for} \quad XPD_g \le 35 \\ 40 & \text{for} \quad XPD_g > 35 \end{cases} \tag{73}$$

where XPD_g is the manufacturer's guaranteed minimum XPD at boresight for both the transmitting and receiving antennas, i.e., the minimum of the transmitting and receiving antenna boresight XPDs.

Step 2: Evaluate the multipath activity parameter:

$$\eta = 1 - e^{-0.2(P_0)^{0.75}} \tag{74}$$

where $P_0 = p_w/100$ is the multipath occurrence factor corresponding to the percentage of the time p_w (%) of exceeding $A = 0$ dB in the average worst month, as calculated from equation (7) or (8), as appropriate.

Step 3: Determine:

$$Q = -10 \log\left(\frac{k_{XP}\ \eta}{P_0}\right) \tag{75}$$

where:

$$k_{XP} = \begin{cases} 0.7 & \text{one transmit antenna} \\ 1 - 0.3 \exp\left[-4 \times 10^{-6}\left(\frac{s_t}{\lambda}\right)^2\right] & \text{two transmit antennas} \end{cases} \tag{76}$$

In the case where two orthogonally polarized transmissions are from different antennas, the vertical separation is s_t (m) and the carrier wavelength is λ (m).

Step 4: Derive the parameter C from:

$$C = XPD_0 + Q \tag{77}$$

Step 5: Calculate the probability of outage P_{XP} due to clear-air cross-polarization from:

$$P_{XP} = P_0 \times 10^{-\frac{M_{XPD}}{10}} \tag{78}$$

where M_{XPD} (dB) is the equivalent XPD margin for a reference BER given by:

$$M_{XPD} = \begin{cases} C - \frac{C_0}{I} & \text{without XPIC} \\ C - \frac{C_0}{I} + XPIF & \text{with XPIC} \end{cases} \tag{79}$$

Here, C_0/I is the carrier-to-interference ratio for a reference BER, which can be evaluated either from simulations or from measurements.

XPIF is a laboratory-measured cross-polarization improvement factor that gives the difference in cross-polar isolation (XPI) at sufficiently large carrier-to-noise ratio (typically 35 dB) and at a specific BER for systems with and without cross polar interference canceller (XPIC). A typical value of XPIF is about 20 dB.

4.2 Prediction of XPD outage due to precipitation effects

4.2.1 XPD statistics during precipitation conditions

Intense rain governs the reductions in XPD observed for small percentages of time. For paths on which more detailed predictions or measurements are not available, a rough estimate of the unconditional distribution of XPD can be obtained from a cumulative distribution of the co-polar attenuation (CPA) for rain (see § 2.4) using the equi-probability relation:

$$XPD = U - V(f) \log CPA \quad \text{dB} \tag{80}$$

The coefficients U and $V(f)$ are in general dependent on a number of variables and empirical parameters, including frequency, f. For line-of-sight paths with small elevation angles and horizontal or vertical polarization, these coefficients may be approximated by:

$$U = U_0 + 30 \log f \tag{81}$$

$$\begin{aligned} V(f) &= 12.8\, f^{0.19} && \text{for} \quad 8 \le f \le 20 \text{ GHz} \\ V(f) &= 22.6 && \text{for} \quad 20 < f \le 35 \text{ GHz} \end{aligned} \tag{82}$$

An average value of U_0 of about 15 dB, with a lower bound of 9 dB for all measurements, has been obtained for attenuations greater than 15 dB.

The variability in the values of U and $V(f)$ is such that the difference between the CPA values for vertical and horizontal polarizations is not significant when evaluating XPD. The user is advised to use the value of CPA for circular polarization when working with equation (80).

Long-term XPD statistics obtained at one frequency can be scaled to another frequency using the semi-empirical formula:

$$XPD_2 = XPD_1 - 20 \log (f_2 / f_1) \quad \text{for} \quad 4 \le f_1, f_2 \le 30 \text{ GHz} \tag{83}$$

where XPD_1 and XPD_2 are the XPD values not exceeded for the same percentage of time at frequencies f_1 and f_2.

The relationship between XPD and CPA is influenced by many factors, including the residual antenna XPD, that has not been taken into account. Equation (82) is least accurate for large differences between the respective frequencies. It is most accurate if XPD_1 and XPD_2 correspond to the same polarization (horizontal or vertical).

4.2.2 Step-by-step procedure for predicting outage due to precipitation effects

Step 1: Determine the path attenuation, $A_{0.01}$ (dB), exceeded for 0.01% of the time from equation (34).

Step 2: Determine the equivalent path attenuation, A_p (dB):

$$A_p = 10^{((U - C_0/I + XPIF)/V)} \tag{84}$$

where U is obtained from equation (81) and V from equation (82), C_0/I (dB) is the carrier-to-interference ratio defined for the reference BER without XPIC, and XPIF (dB) is the cross-polarized improvement factor for the reference BER.

If an XPIC device is not used, set XPIF = 0.

Step 3: Determine the following parameters:

$$m = \begin{cases} 23.26 \log \left[A_p / \, 0.12 \, A_{0.01} \right] & \text{if } m \le 40 \\ 40 & \text{otherwise} \end{cases} \tag{85}$$

and

$$n = \left(-12.7 + \sqrt{161.23 - 4m} \right) \Big/ 2 \tag{86}$$

Valid values for n must be in the range of –3 to 0. Note that in some cases, especially when an XPIC device is used, values of n less than –3 may be obtained. If this is the case, it should be noted that values of p less than –3 will give outage BER $< 1 \times 10^{-5}$.

Step 4: Determine the outage probability from:

$$P_{XPR} = 10^{(n-2)} \tag{87}$$

5 Distortion due to propagation effects

The primary cause of distortion on line-of-sight links in the UHF and SHF bands is the frequency dependence of amplitude and group delay during clear-air multipath conditions. In analogue systems, an increase in fade margin will improve the performance since the impact of thermal noise is reduced. In digital systems, however, the use of a larger fade margin will not help if it is the frequency selective fading that causes the performance reduction.

The propagation channel is most often modelled by assuming that the signal follows several paths, or rays, from the transmitter to the receiver. These involve the direct path through the atmosphere and may include one or more additional ground-reflected and/or atmospheric refracted paths. If the direct signal and a significantly delayed replica of near equal amplitude reach the receiver, inter symbol interference occurs that may result in an error in detecting the information. Performance prediction methods make use of such a multi-ray model by integrating the various variables such as delay (time difference between the first arrived ray and the others) and amplitude distributions along with a proper model of equipment elements such as modulators, equalizer, forward-error correction (FEC) schemes, etc. Although many methods exist, they can be grouped into three general classes based on the use of a system signature, linear amplitude distortion (LAD), or net fade margin. The signature approach often makes use of a laboratory two-ray simulator model, and connects this to other information such as multipath occurrence and link characteristics. The LAD approach estimates the distortion distribution on a given path that would be observed at two frequencies in the radio band and makes use of modulator and equalizer characteristics, etc.

Similarly, the net-fade margin approach employs estimated statistical distributions of ray amplitudes as well as equipment information, much as in the LAD approach. In § 5.1, the method recommended for predicting error performance is a signature method.

Distortion resulting from precipitation is believed to be negligible, and in any case a much less significant problem than precipitation attenuation itself. Distortion is known to occur in millimetre and sub-millimetre wave absorption bands, but its effect on operational systems is not yet clear.

5.1 Prediction of outage in unprotected digital systems

The outage probability is here defined as the probability that BER is larger than a given threshold.

Step 1: Calculate the mean time delay from:

$$\tau_m = 0.7 \left(\frac{d}{50} \right)^{1.3} \quad \text{ns} \tag{88}$$

where d is the path length (km).

Step 2: Calculate the multipath activity parameter η as in Step 2 of § 4.1.

Step 3: Calculate the selective outage probability from:

$$P_s = 2.15\eta \left(W_M \times 10^{-B_M / 20} \frac{\tau_m^2}{|\tau_{r,\,M}|} + W_{NM} \times 10^{-B_{NM} / 20} \frac{\tau_m^2}{|\tau_{r,NM}|} \right) \tag{89}$$

where:

W_x: signature width (GHz)

B_x: signature depth (dB)

$\tau_{r,x}$: the reference delay (ns) used to obtain the signature, with x denoting either minimum phase (M) or non-minimum phase (NM) fades.

If only the normalized system parameter K_n is available, the selective outage probability in equation (89) can be calculated by:

$$P_s = 2.15\eta \, (K_{n,M} + K_{n,NM}) \frac{\tau_m^2}{T^2} \tag{90}$$

where:

T: system baud period (ns)

$K_{n,x}$: the normalized system parameter, with x denoting either minimum phase (M) or non-minimum phase (NM) fades.

The signature parameter definitions and specification of how to obtain the signature are given in Recommendation ITU-R F.1093.

6 Techniques for alleviating the effects of multipath propagation

The effects of slow relatively non-frequency selective fading (i.e. flat fading) due to beam spreading, and faster frequency-selective fading due to multipath propagation must both be taken into account in link design. There are a number of techniques available for alleviating these effects, most of which alleviate both at the same time. The same techniques often alleviate the reductions in cross-polarization discrimination also. They can be categorized as techniques that do not require some kind of diversity reception or transmission, and techniques that do require diversity.

Since it is desirable for economic reasons to avoid diversity whenever possible, strategies and techniques that do not require diversity are considered first in § 6.1. These strategies and techniques are also relevant for diversity systems, however, and should be employed when convenient even though they may be less necessary. Diversity techniques are discussed in § 6.2.

6.1 Techniques without diversity

In order to reduce the effects of multipath fading without diversity there are several techniques that can be employed either if the link is between existing towers or between new towers to be built. It is useful to consider these techniques as accomplishing one or more of the following Strategies:

Strategy A: reducing the occurrence of significant flat fading due to atmospheric mechanisms (beam spreading, antenna decoupling, and atmospheric multipath; see § 2.3);

Strategy B: reducing the occurrence of significant surface reflections;

Strategy C: reducing the relative delay of the surface reflections with respect to the atmospheric wave.

6.1.1 Increase of path inclination

Links should be sited to take advantage of rough terrain in ways that will increase the path inclination (sometimes referred to as the high-low technique), since it tends to accomplish Strategy A above and to some extent Strategy B also. This approach should be conducted jointly with more specific efforts to use shielding from terrain to reduce the levels of surface reflection (Strategy B; see § 6.1.2), since the two are closely connected.

Where towers are already in place, antenna height at one end of the path could be reduced to accomplish this so long as the clearance rules in § 2.2.2 are satisfied.

6.1.2 Reduction of effect of surface reflections

Links should be sited where possible to reduce the occurrence of significant specular and diffuse surface reflections (or at least change large specular reflections into smaller diffuse reflections), thus reducing the occurrence of surface multipath fading and distortion (Strategy B). There are several techniques for doing this, most of which are related to one another. Therefore, application of one should not be carried out without also considering the others. The techniques are as follows:

6.1.2.1 Shielding of the reflection point

One technique is to use the advantage of hills, mountains or buildings along the path to shield the antennas from the more specularly-reflective surfaces along the path (e.g. water surfaces, plains, smooth hilltops not covered by trees, building tops; see Fig. 8). Ideally, hills or mountains should be covered in vegetation to further reduce the level of the field diffracted over them. Of course, shielding of reflective surfaces is more readily possible when path clearance is reduced (see § 6.1.3).

FIGURE 8

Example of shielding of antenna from specular reflection

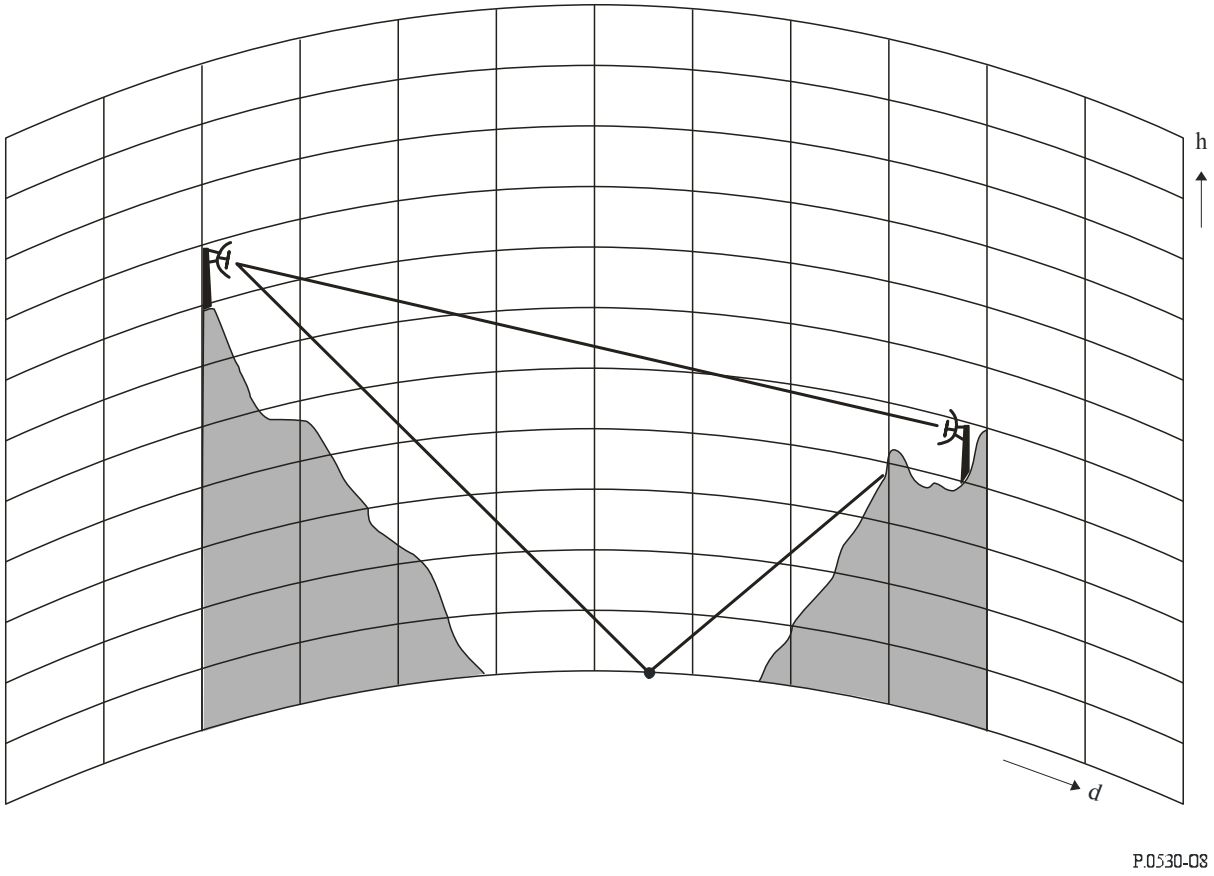

Ray-tracing analyses to find a suitable shielding obstacle should be carried out for a range of effective k factors varying from k_e (99.9%) (or some other minimum value) to infinity (see § 2.2.2). Care must be taken to ensure that the surface reflection is blocked, or at least partially shielded, for large effective k values, as well as the median value. Clearly the advantage of obstacle shielding is lost to some extent if one or more surface reflected waves are super-refracted over the obstacles, since surface multipath fading and distortion are more likely to occur during such conditions. Care must also be taken to ensure that the direct wave is not diffracted more than acceptable within the path clearance criteria at the low effective k values occurring in sub-refractive conditions.

6.1.2.2 Moving of reflection point to poorer reflecting surface

Another technique is to adjust the antenna height at one or both ends of the path to place reflections on a rougher terrain or vegetative surface than would otherwise be possible. On overwater paths, for example, the path inclination might be adjusted to place the surface reflection on a land surface rather than on water, and even better, on a land surface covered by trees or other vegetation. The reflection point moves towards an antenna that is being lowered and away from an antenna that is being raised.

The method for determining the location of possible reflection areas is given in § 6.1.2.3 (Steps 1 to 3). On sufficiently short paths, the full technique should be employed to see if one or both antenna heights can be chosen so as to avoid destructive interference from specular surface reflections.

Methods for calculating or measuring the strength of a surface specular reflection are given in § 6.1.2.4.

6.1.2.3 Optimum choice of antenna heights

On sufficiently short paths the height of one or both antennas can sometimes be adjusted so that any surface reflected wave(s) does not interfere destructively with the direct wave over the significant range of effective k values. As noted in § 6.1.2.2, adjustment of antenna heights may also be used to place reflections on a more poorly reflecting surface. The step-by-step procedure for applying both techniques, and determining if diversity is necessary, is as follows:

Step 1: Calculate the tentative heights of the transmitting and receiving antennas using the clearance rule for non-diversity systems in § 2.2.2.1.

Step 2: Calculate the heights of the transmitting and upper receiving antennas above possible specular reflection areas on or near the path profile. Such areas as bodies of water, plains, the smooth top of a hill not covered by trees, or the tops of buildings can cause significant specular reflections. Such areas of course may or may not be horizontal, and there may be more than one of them (see Note 1). While some areas can be determined from maps, others may require a detailed inspection of the terrain along and in the close vicinity of the path.

The heights h_1 and h_2 of the antennas above a reflection area of inclination angle ν (see Note 1) are as follows (see Fig. 9):

$$h_1 = h_{1G} + y_1 - y_0 + x_0 \times 10^3 \times \tan \nu \quad \text{m} \tag{91}$$

$$h_2 = h_{2G} + y_2 - y_0 - (d - x_0) \times 10^3 \times \tan \nu \quad \text{m} \tag{92}$$

where:

y_1, y_2: altitudes of ground above sea level at sites 1 and 2, respectively (m)

h_{1G}, h_{2G}: heights of antennas above ground at sites 1 and 2, respectively (m)

y_0: altitude of mid-point of reflection area above sea level (m)

x_0: distance of mid-point of reflection area from site 1 (km).

If the reflection area is on the sea, account needs to be taken of the tidal variations.

FIGURE 9

Path with reflective terrain

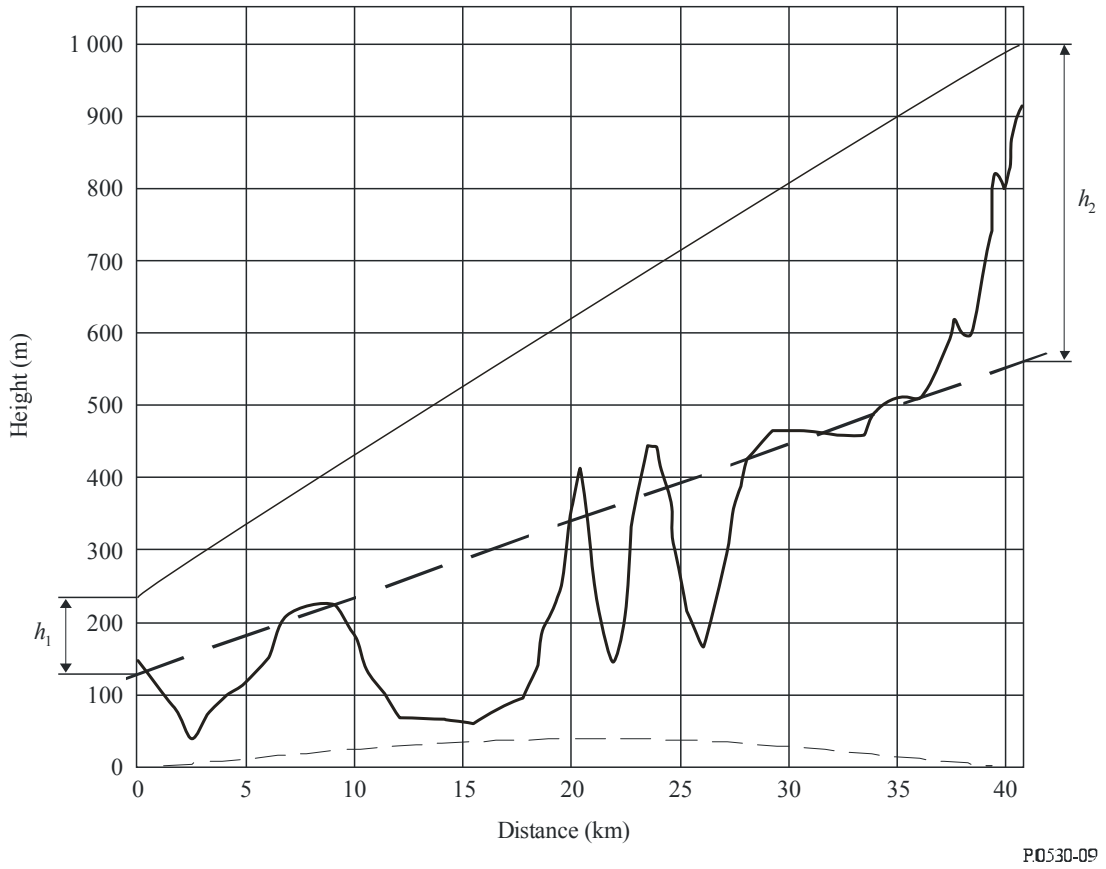

Step 3: For a range of effective k factors varying from k_e (99.9%) to infinity (see § 2.2.2; in practice, a large value of k can be chosen such as $k = 1.0 \times 10^9$), calculate the distances d_1 and d_2 of each possible reflecting surface from sites 1 and 2, respectively, from (see Note 2):

$$d_1 = d(1 + b)/2 \quad \text{km} \tag{93}$$

$$d_2 = d(1 - b)/2 \quad \text{km} \tag{94}$$

where:

$$b = 2\sqrt{\frac{m+1}{3m}}\cos\left[\frac{\pi}{3} + \frac{1}{3}\arccos\left(\frac{3c}{2}\sqrt{\frac{3m}{(m+1)^3}}\right)\right] \tag{95}$$

$$m = \frac{d^2}{4a_e(h_1 + h_2)} \times 10^3 \tag{96}$$

$$c = (h_1 - h_2)/(h_1 + h_2) \tag{97}$$

with $a_e = ka$ the effective radius of the Earth for a given k factor (a = 6 375 km being the actual radius of the Earth); in equation (96), d is in kilometres and h_1 and h_2 in metres.

If specular reflection areas can be avoided by adjusting one or both antenna heights by reasonable amounts, while staying within the clearance rules (Step 1), estimate the change and start again at Step 2.

Step 4: For specularly reflecting surfaces that cannot be avoided, calculate the path length difference between the directed and reflected waves (or rays) in wavelengths for the same range of effective k values from:

$$\tau = \frac{2f}{0.3d}\left[h_1 - \frac{d_1^2}{12.74k}\right]\left[h_2 - \frac{d_2^2}{12.74k}\right]\times 10^{-3} \quad (98)$$

Each time the number of wavelengths, τ, is a positive integer as k varies (i.e. 1, 2, etc.), the received signal level passes through a minimum. This condition must be avoided as much as possible. The greater the number of integer values of $\tau_{max} - \tau_{min}$ as k varies over its range, the more likely is the performance to be compromised and some kind of diversity necessary.

If $\tau_{max} - \tau_{min} < 1$ as k varies over the relevant range, diversity can almost certainly be avoided. However, on paths greater than about 7.5 km in length, the best way to ensure that diversity protection is not necessary is to apply the procedure for calculating multipath occurrence in § 2.3, and the outage prediction procedure for unprotected digital systems in § 5.1. In any case, the heights of one or both antennas should be adjusted so that $\tau \approx 0.5$ at the median value of k.

If $\tau_{max} - \tau_{min} \geq 1$, the depth of surface multipath fades and whether some kind of diversity might be necessary depends on how well the signal is reflected (see § 6.1.2.2 and 6.1.2.3) and whether there is significant discrimination against surface reflections from one or both of the antennas (see § 6.1.2.5). However, it must be remembered that, on sufficiently long paths, abnormal layers with extremely negative refractivity gradients can cause the direct wave to fade as a result of beam spreading and that the surface reflected wave(s) can be simultaneously enhanced as a result of energy diverted from the direct wave in the direction of the surface. The best way to determine whether some kind of diversity protection is necessary is to apply the procedure for calculating multipath occurrence in § 2.3, and the outage prediction procedure for unprotected digital systems in § 5.1.

NOTE 1 – Since the path profile is based on sample heights a certain distance apart, the actual terrain slope will vary somewhat between the sample points on the profile. It is suggested that a small variation in the inclination angle ν about the value estimated from the digital profile be allowed (e.g. values corresponding to changes in profile heights at one end of the profile segment concerned by ±10 m). If necessary, a visual inspection of the path between the sample terrain points can be carried out.

In some cases where the path profile is somewhat rough and its treatment in individual path segments does not seem appropriate, then a regression curve should be placed through the path profile in the manner discussed in § 6.1.2.4.1 and reflection be considered to occur from this curve in order to calculate the heights above and distances to the reflecting point. In such a case, the steps of this subsection and § 6.1.2.4.1 need to be considered in combination.

NOTE 2 – For some designs, it may be desirable to use a minimum effective k value smaller than k_e (99.9%).

6.1.2.4 Choice of vertical polarization

On overwater paths at frequencies above about 3 GHz, it is advantageous to choose vertical polarization over horizontal polarization. At grazing angles greater than about 0.7°, a reduction in the surface reflection of 2-17 dB can be expected over that at horizontal polarization.

A more exact estimate of the effective reflection coefficient of the surface area involved in a specular reflection can be obtained either by a calculation or measurement, as follows:

6.1.2.4.1 Calculation of effective surface reflection coefficient

The effective reflection coefficient of the surface can be calculated from the following step-by-step procedure (see Note 1):

Step 1: Calculate the complex permittivity of the Earth's surface in the vicinity of the surface reflection areas from:

$$\eta = \varepsilon_r - j18\sigma/f \tag{99}$$

where ε_r is the relative permittivity and σ is the conductivity (S/m). Estimate ε_r and σ from the information given in Recommendation ITU-R P.527.

Step 2: Calculate the grazing angle for the range of effective k values obtained in Step 3 of § 6.1.2.3 from:

$$\varphi = \frac{h_1 + h_2}{d}\left[1 - m\left(1 + b^2\right)\right] \tag{100}$$

Step 3: Calculate the reflection coefficient of the surface and the same range of k values from:

$$\rho = \left| \frac{\sin\varphi - \sqrt{C}}{\sin\varphi + \sqrt{C}} \right| \tag{101}$$

where:

$$C = \eta - \cos^2\varphi \qquad \text{horizontal polarization} \tag{102}$$

$$C = \frac{\eta - \cos^2\varphi}{\eta^2} \qquad \text{vertical polarization} \tag{103}$$

Step 4: Calculate the divergence factor of the Earth's surface from:

$$D = \sqrt{\frac{1 - m(1 + b^2)}{1 + m(1 - 3b^2)}} \tag{104}$$

Step 5: Calculate the length, L_1, of the 1st Fresnel zone ellipse on the Earth's surface along the path from:

$$L_1 = d\sqrt{1 + \frac{4 f h_1 h_2 \times 10^{-2}}{3d}}\left[1 + \frac{f(h_1 + h_2)^2 \times 10^{-2}}{3d}\right]^{-1} \quad \text{km} \tag{105}$$

and the width, W_1, in the transverse direction from:

$$W_1 = \sqrt{\frac{3 \times 10^{-4} d}{f}} \quad \text{km} \tag{106}$$

where h_1 and h_2 are in metres and d in kilometres. Assume that the 1st Fresnel zone ellipse is centred at the geometric point of reflection of an obvious surface reflection (see Note 2).

Step 6: If there is clearly only a portion(s) of the 1st Fresnel ellipse that will be specularly reflecting, estimate the length Δx (km) of this portion. Then estimate the specular-reflection factor from (see Note 2):

$$R_s = \sqrt{\frac{f(h_1 + h_2)^4 \, (\Delta x)^2 \times 10^{-2}}{3 h_1 h_2 d^3}} \tag{107}$$

where again h_1 and h_2 are in metres and d in kilometres. Otherwise, assume that $R_s = 1$.

Step 7: If the surface within the 1st Fresnel ellipse is somewhat rough, estimate the surface roughness factor from:

$$R_r = \sqrt{\frac{1 + (g^2 / 2)}{1 + 2.35(g^2 / 2) + 2\pi (g^2 / 2)^2}} \tag{108}$$

where:

$$g = \frac{40 \pi f \sigma_h \sin\varphi}{3} \tag{109}$$

with σ_h (m) the standard deviation of surface height about the regression curve through that portion of the path profile within the 1st Fresnel ellipse (see Note 3). Otherwise, assume that $R_r = 1$.

Step 8: Calculate the effective reflection coefficient for the relevant range of effective k values from:

$$\rho_{eff} = \rho D R_s R_r \tag{110}$$

The level of the reflected wave(s) relative to the direct wave can then be estimated by the technique given in § 6.1.2.5.

NOTE 1 – It is recognized that it will be difficult on many overland paths (particularly at higher frequencies) to obtain an accurate estimate of the effective surface reflection coefficient because of various uncertainties such as the surface conductivity, surface roughness, etc., and the degree of subjectivity currently needed to obtain a calculation. The calculation procedure may only be a rough guide in such situations to help identify problem paths or to help choose one path from another, even if this possibility exists in the first place. For surface reflection on ground, it may be desirable to assume wet ground in areas in which this is prevalent during the same hours and months in which fading is prevalent.

NOTE 2 – Equation (107) is most accurate if neither edge of the specularly-reflecting area is far from the point of specular reflection. In some cases it may be best to categorize the 1st Fresnel zone area into a very rough portion which is clearly not reflecting (because of the steep angle of terrain involved or because of terrain shielding), and another less rough portion which is partially reflecting, but for which a surface roughness factor calculation is carried out in the manner of Step 7.

By way of guidance, if the reflecting area of the Earth's surface covers exactly the area of the 1st Fresnel zone along the path, the amplitude of the reflected wave is 2.6 dB greater than that of the direct wave (not taking into account the effect of the divergence factor D and the antenna discrimination discussed in § 6.1.2.5). This figure would be 6 dB if the reflecting area covered exactly the 1st Fresnel zone not only longitudinally, but also laterally. On the other hand, if the reflecting area does not contain the geometric point of reflection, the relative amplitude of the reflected wave will not be greater than −3.4 dB. If the reflecting area is completely outside the 1st Fresnel zone, the relative amplitude of the reflected wave will be less than −11.5 dB.

NOTE 3 – If the path profile is sufficiently rough, it may be best to pass a regression curve through the profile along a length corresponding to the length of the 1st Fresnel zone itself in order to serve as a basis for determining the location of the reflection point and subsequent calculation of the standard deviation of profile heights σ_h (m) about this curve. Since the initial location of the 1st Fresnel zone is unknown this may be an iterative process. If the 1st Fresnel ellipse is on water, a smooth surface should be assumed.

6.1.2.4.2 Measurement of effective surface reflection coefficient

The effective reflection coefficient of the reflecting surface can be measured in normal propagation conditions (see § 8 for the best time of day; see also Note 1) by obtaining a height-gain pattern of the received signal level as either the transmitting antenna or the receiving antenna is adjusted in height over a sufficient enough range that both maxima and minima in the pattern are observed. If ΔE (dB) is the difference between maximum and minimum levels (see Fig. 10), the effective reflection coefficient is given by:

$$\rho_{eff} = \frac{10^{\Delta E/10} + 1 - 2 \times 10^{\Delta E/20}}{10^{\Delta E/10} - 1} \tag{111}$$

NOTE 1 – The ground surface may be drier during the part of the day when normal propagation conditions are expected than it is during the part of the day when multipath conditions are expected. It may be desirable in such situations to introduce a correction based on the equations in § 6.1.2.4.1 and the known differences of ground conductivity in wet and dry conditions. The material in § 6.1.2.4.1 and 6.1.2.4.2 is intended to be a rough guide only.

FIGURE 10

Measurement of ΔE (dB) from height gain pattern

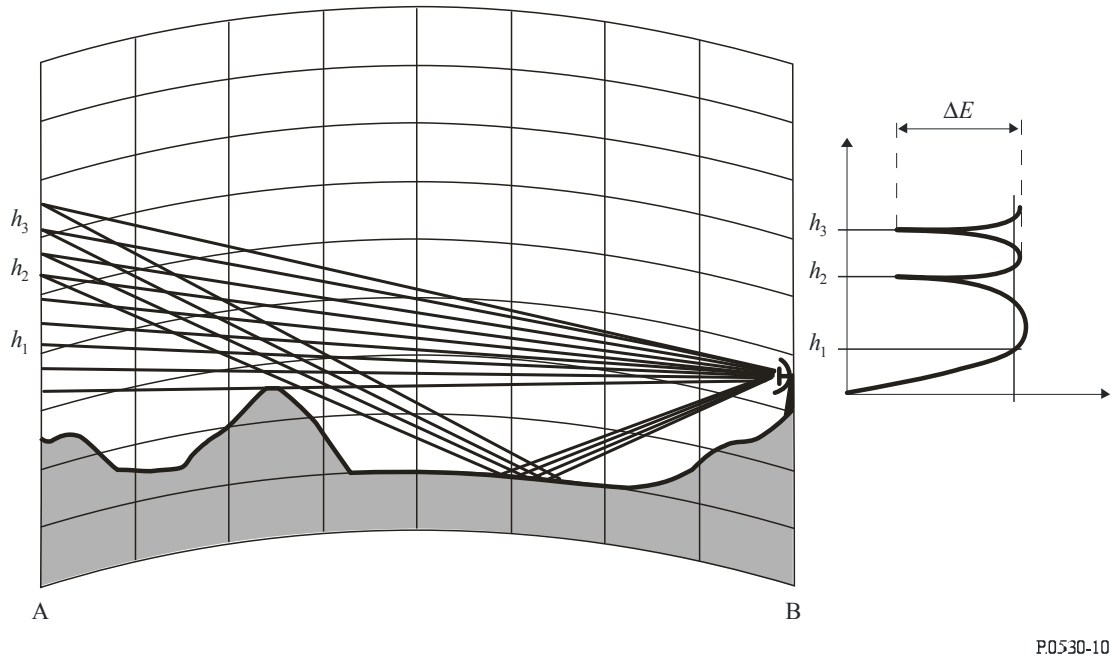

6.1.2.5 Use of antenna discrimination

On sufficiently inclined paths or paths with naturally large clearance, the angles between the direct and surface-reflected wave(s) become large enough to take advantage of the radiation pattern of one or both antennas to discriminate against the reflected wave(s). Even without this natural advantage, it can be advantageous to tilt one or both antennas slightly upwards to increase the amount of discrimination available. The step-by-step procedure is as follows:

Step 1: Calculate the angles between the direct and surface reflected wave(s) at sites 1 and 2 for the relevant range of effective k values obtained in Step 3 of § 6.1.2.4 from:

$$\alpha_1 = \frac{180}{\pi}\left[\frac{h_1}{d_1} - \frac{h_1 - h_2}{d} - \frac{d_2}{12.74k}\right]\times 10^{-3} \quad \text{degrees} \tag{112}$$

$$\alpha_2 = \frac{180}{\pi}\left[\frac{h_2}{d_2} - \frac{h_2 - h_1}{d} - \frac{d_1}{12.74k}\right]\times 10^{-3} \quad \text{degrees} \tag{113}$$

Step 2: Estimate the loss in level of the surface reflected signal(s) relative to the direct signal introduced by antenna discrimination from (see Note 1):

$$L_a = 12\left[\left(\frac{\alpha_1}{\alpha_{a1}}\right)^2 + \left(\frac{\alpha_2}{\alpha_{a2}}\right)^2\right] \quad \text{dB} \tag{114}$$

where α_{a1} and α_{a2} are the half-power beamwidths of the antennas.

If the surface-reflected wave(s) leaves and enters within the half-width of one or both antennas, the relevant antennas should normally be tilted upwards by about half a beamwidth so as to introduce additional antenna discrimination (see Note 2). Even if the angles-of-arrival of the surface-reflected wave are a little outside the half-width of the antennas, a small upward tilt could be advantageous (see Note 2). The total loss due to antenna discrimination can then be estimated from (see Note 1):

$$L_a = 12\left[\left(\frac{\alpha_1 + \alpha_{t1}}{\alpha_{a1}}\right)^2 + \left(\frac{\alpha_2 + \alpha_{t2}}{\alpha_{a2}}\right)^2\right] \quad \text{dB} \tag{115}$$

where α_{t1} and α_{t2} are the angles with which the antennas are tilted upwards.

Step 3: It may be useful on some paths to estimate or measure the effective surface reflection coefficient so as to obtain an overall estimate of the level of the surface reflection(s) in normal propagation conditions. This can be done using the information in § 6.1.2.4. The overall loss in level of the surface reflected wave(s) is then given by:

$$L_s = L_a - 20\log\rho_{eff} \quad \text{dB} \tag{116}$$

where L_a is obtained from equation (114) or (115), as appropriate. Since the effective surface reflection coefficient can be enhanced in surface-multipath conditions, however, it is not critical to estimate its value exactly or at all in order to calculate appropriate upward tilt angles for the antennas (see Step 5).

Step 4: If one or both antennas are tilted upwards, the corresponding loss in level of the direct signal in normal propagation conditions (k = 4/3) is given by (see Note 1):

$$L_d(k=4/3) = 12\left[\left(\frac{\alpha_{t1}}{\alpha_{a1}}\right)^2 + \left(\frac{\alpha_{t2}}{\alpha_{a2}}\right)^2\right] \quad \text{dB} \tag{117}$$

In super- or sub-refractive conditions, $L_d(k)$ can be estimated from (see Note 1):

$$L_d(k) = 12\left[\left(\frac{\alpha_{t1}-\alpha_d}{\alpha_{a1}}\right)^2 + \left(\frac{\alpha_{t2}-\alpha_d}{\alpha_{a2}}\right)^2\right] \quad \text{dB} \tag{118}$$

where the angle-of-arrival of the direct signal is given approximately by (see Note 2):

$$\alpha_d = -0.0045d\left(\frac{1}{k} - \frac{3}{4}\right) \quad \text{degrees} \tag{119}$$

Step 5: The maximum possible fade depth in normal propagation conditions (k = 4/3) from destructive interference between the direct and surface-reflected signals can be calculated from:

$$A_{max} = -20\log\left(10^{-L_d/20} - 10^{-L_s/20}\right) \quad \text{dB} \tag{120}$$

where L_d is given by equation (117) and L_s by equation (116) (see Note 2). In super-refractive or sub-refractive conditions in which the direct signal also undergoes an additional loss $0.5L_{add}$ (e.g. due to beam spreading in super-refractive conditions) and the surface-reflected signal a gain $-0.5L_{add}$, the maximum possible fade depth is given by:

$$A_{max} = -20\log\left(10^{-(L_d+0.5L_{add})/20} - 10^{-(L_s-0.5L_{add})/20}\right) \quad \text{dB} \tag{121}$$

where L_d is given by equation (118) and L_s by equation (116) (see Note 2).

The tilt angles of the antennas can be optimized to minimize surface multipath fading or surface multipath amplitude distortion, or a combination of the two. Optimization to minimize fading can be accomplished by setting the value of L_{add} in equation (121) such that L_d is less than L_s at $k = \infty$ (in practice, a large value of k can be chosen such as $k = 1 \times 10^9$) by about 0.3 dB and minimizing A_{max} by trial-and-error choice of the tilt angles. Alternatively, the value of ρ_{eff} in equation (116) can be set equal to a value approaching 1.0 or larger so as to accomplish the same difference of about 0.3 dB (see Note 2), and then the optimization carried out. This avoids the situation where ρ_{eff} is not known. Loss of fade margin by this approach is in the range 2.5-4 dB.

Optimization to minimize amplitude distortion due to surface multipath can be accomplished by increasing the tilt angles still further until the relative antenna discrimination against the surface reflected wave(s) is maximized. This will be accomplished when the difference in discrimination between the direct and surface-reflected waves is maximum. However, in order to accurately optimize the tilt angles against surface multipath distortion, the antenna patterns must be available since the model of equation (115) is less accurate outside the half-widths of the antennas, especially as the edge of the main lobe is approached (see Note 1). Since optimization against amplitude distortion is accomplished against the further loss of flat fade margin, it is recommended that the tilt angles obtained by the optimization against fading be increased by the same proportions until a

maximum loss of fade margin of about 6 dB occurs. Although the resulting tilt angles are less optimal against fading itself, the increase in fade depth is only a fraction of a decibel (see Note 3).

It should be noted that optimal discrimination against surface multipath by antenna uptilting will also tend to discriminate against atmospheric multipath (see Note 4).

NOTE 1 – This Gaussian-beam approximation is most accurate within the beamwidths of the antennas. Outside the beamwidths, the actual patterns can be used to obtain a more accurate estimate if desired. This is especially important as the edge of the main lobe is approached.

NOTE 2 – Upward tilting of the antennas is desirable for improved performance in surface multipath fading conditions, regardless of the level of the surface-reflected wave(s) in normal propagation conditions (i.e. $k = 4/3$). The objective in optimizing to minimize fading is to reduce the level of the surface-reflected waves(s) by a larger amount than that of the direct wave, while reducing the latter only enough that the overall fade depth is minimized. The objective in optimizing to minimize amplitude distortion is to maximize the relative difference between the amplitudes of the direct and surface-reflected wave(s) at the expense of increasing the maximum fade depth slightly. Both can be accomplished by moving the angle-of-arrival of the surface reflected wave(s) to points on the antenna patterns where they are steeper. If necessary, the loss of flat-fade margin in normal conditions from the loss in antenna discrimination in the direction of the direct wave due to upward tilting can be compensated by increasing the size of the antennas.

Antenna tilt angles to minimize the effect of the surface reflection(s) in normal propagation conditions will vary depending on the path geometry, the antenna beamwidths, and the relative level of the surface reflection(s). Although the larger the beamwidth, the larger the tilt angle required to have an effect in normal propagation conditions, the appropriate ratio of tilt angle to beamwidth will become smaller with increasing beamwidth.

The antenna tilt angles to minimize the effect of the surface reflection(s) in surface multipath conditions will be larger than those for normal conditions, and should usually be the ones chosen. When an extreme layer such as a duct causes a beam-spreading loss in the direct signal level, there is an increased likelihood that the surface-reflected signal(s) will be simultaneously enhanced and a significant multipath fade will result. This will be accompanied by an increase in propagation distortion.

For the purpose of choosing appropriate tilt angles to minimize fade depth based on equation (121), simulation can be carried out in the manner described in Step 5. (Whether L_d and L_s are caused to approach one another within 0.3 dB by changing one or the other, or both simultaneously, seems not to be a critical factor to the result.) The optimum tilt angles will vary depending on the angles of the surface-reflected waves as given by equations (112) and (113). The larger of the antenna tilt angles corresponds to the larger angle of surface reflection from this antenna. As noted, typical loss of margin for optimal tilt angles is in the 2.5-4 dB range. In any case, if the antenna sizes are increased to compensate for loss in flat fade margin, another optimization must take place to determine the new optimal tilt angles.

As noted, optimization to minimize amplitude distortion should be preceded by the step to minimize fading and the tilt angles increased by equal proportions. Whether one set of tilt angles is used, the other, or something in between will depend on system considerations (see Note 3).

Note that during surface multipath conditions some of the loss of antenna discrimination in the direction of the strongest ray (normally the direct wave) as a result of antenna tilting is regained by the fact that this ray tends to have a positive angle-of-arrival.

NOTE 3 – If an increase in antenna size can be avoided by optimizing the antenna tilt angles to minimize the maximum fade depth (with the attendant loss in flat fade margin of 2.5-4 dB), this may be the best alternative. On the other hand, if optimizing tilt angles to minimize amplitude distortion will improve performance sufficiently to avoid diversity, this may be the best alternative. The choice will depend on the quality of equalization used in the system. A third alternative would be to choose antenna tilt angles that result in a loss of flat fade margin somewhere in between the extremes of 2.5-4 dB and about 6 dB. It is important to observe that in optimization to minimize distortion, there is only a small departure from the optimal fading condition (i.e. minimum fade depth).

NOTE 4 – Both ray-tracing analyses and extensive experimental measurements of the angles-of-arrival and amplitudes of the three strongest multipath waves indicate that the atmospheric multipath wave with the larger upward angle-of-arrival tends to be higher in level than the second strongest atmospheric multipath

wave. This indicates that as long as the antennas are set to upward tilt angles larger than this larger of the two angles-of-arrival (typically less than 0.3° for paths lengths in the range 31-51 km), antenna discrimination against atmospheric multipath will also increase. Thus, optimal antenna uptilting should normally be based on minimizing the effects of surface multipath.

6.1.3 Reduction of path clearance

Another technique that is not quite as well understood or as quantified as the others involves the reduction of path clearance to incur a predictable amount of diffraction loss, at least in sub-refractive conditions. This technique is believed to work in large part by:

– reducing the likelihood and/or severity of beam-spreading loss suffered by the direct wave from an extreme layer (such as a duct) occurring just below or partially below the full length of the path (a Strategy A technique);

– simultaneously reducing the likelihood that the same layer will enhance surface reflections (a Strategy B technique).

This in turn reduces the likelihood that the direct wave will combine destructively with one or more surface reflections to cause severe frequency selective fading.

Another means by which the technique is believed to work is that the delays between the direct wave and the interfering surface-reflected wave(s) are reduced if the extreme layer causing the beam spreading of the direct wave is only partially below the path (i.e. Strategy C). Consequently, this results in less severe frequency selective fading than if the entire layer were below the path.

This technique requires a tradeoff between the reduction of the effects of surface multipath fading on the one hand and increased fading due to diffraction loss in sub-refractive conditions on the other. The path clearance rule in § 2.2.2.1 is designed to avoid diffraction loss in normal refractivity conditions (i.e. median effective k factor), but to allow about 6 dB of diffraction loss in conditions corresponding to k_e (99.9%). In principle, for systems with sufficiently large flat fade margins, larger amounts of diffraction loss could be tolerated in both normal and sub-refractive conditions.

The technique is of greatest value on paths with little or no inclination. However, even on paths with some inclination, it may be useful to reduce path clearance to further reduce the effects of surface multipath.

The technique is more safely applied to the lower antenna in a space-diversity configuration, and it is recommended as a matter of course in the technique presented in § 6.2.1.

6.2 Diversity techniques

Diversity techniques include space, angle and frequency diversity. Normally the use of frequency diversity should be avoided in favour of space diversity, angle diversity, or a combination of the two. Not only is the frequency spectrum used more efficiently in this manner, but also these techniques are generally superior. Space diversity, in particular, helps to combat flat fading (such as caused by beam spreading loss, not by atmospheric multipath with short relative delay) as well as frequency selective fading, whereas frequency diversity only helps to combat frequency selective fading (such as caused by surface multipath and/or atmospheric multipath). Frequency diversity should be avoided whenever possible so as to conserve spectrum. Whenever space diversity is used, angle diversity should also be employed by tilting the antennas at different upward angles. Angle diversity can be used in situations in which adequate space diversity is not possible or to reduce tower heights.

The degree of improvement afforded by all of these techniques depends on the extent to which the signals in the diversity branches of the system are uncorrelated. For narrow-band analogue systems, it is sufficient to determine the improvement in the statistics of fade depth at a single frequency.

For wideband digital systems, the diversity improvement also depends on the statistics of in-band distortion.

The diversity improvement factor, I, for fade depth, A, is defined by:

$$I = p(A) / p_d(A) \tag{122}$$

where $p_d(A)$ is the percentage of time in the combined diversity signal branch with fade depth larger than A and $p(A)$ is the percentage for the unprotected path. The diversity improvement factor for digital systems is defined by the ratio of the exceedance times for a given BER with and without diversity.

6.2.1 Antenna spacing in space diversity systems

The appropriate spacing of antennas in space diversity systems is governed by three factors:

– the need to keep clearance of the lower antenna as low as possible (within the clearance guidelines of § 2.2.2) so as to minimize the occurrence of surface multipath fading (see § 6.1.3);

– the need to obtain a specified space diversity improvement factor for overland paths (see § 6.2.2);

– the need to minimize the chance that the signal on one diversity antenna will be faded by surface multipath when that on the other antenna is faded.

The step-by-step procedure to determine spacing is as follows:

Steps 1-4: Apply Steps 1-4 of § 6.1.2.3 to determine if:

– there are any path areas where a specular surface reflection might be significant; and if

– space diversity to combat surface multipath fading is necessary.

(For two-leg passive-reflector hops with one or more passive reflectors in close proximity, see Note 1.) If there are no significant surface specular reflection areas, go to Step 8.

Step 5: For the same range of effective k values in Step 3, calculate the distances between the adjacent minima, or, maxima, in received signal level (due to interference between the direct wave and the surface multipath wave; see Fig. 10) from:

$$\theta_2 = \frac{150d}{f\left(h_1 - d_1^2 / 12.74k\right)} \quad \text{m} \tag{123}$$

The distance θ_1 at site 1 can be calculated by replacing h_1 and d_1 in equation (123) by h_2 and d_2, respectively.

Carry out this step for each possible specular reflection area.

Step 6: Calculate the possible optimum spacings of the diversity antennas for the same range of k values, from:

$$S_1 = \theta_1 / 2,\ 3\theta_1 / 2,\ 5\theta_1 / 2 \text{ etc.} \quad S_2 = \theta_2 / 2,\ 3\theta_2 / 2,\ 5\theta_2 / 2 \text{ etc.} \quad \text{m} \tag{124}$$

Again, carry out this step for each possible specular reflection area.

Step 7: paths with obvious specular surface reflections: Calculate a tentative height of the diversity antenna from Steps 2-3 of § 2.2.2.2, and the resultant tentative spacing S_1' of the antennas. Compare the tentative spacing with the optimum spacings obtained in Step 6 for the relevant range of effective k values.

For paths for which the level of the surface-reflected signal level is expected to approach that of the direct signal in normal refractivity conditions (i.e. median k or k = 4/3), the minimum optimum spacing obtained in Step 6 (i.e. $S_1 = \theta_1 / 2$) for the median value of k should be chosen as the actual spacing (see Note 2). This will give space diversity protection for the largest range of k values. (At low frequencies, it may be necessary to increase the height of the upper antenna to accomplish even this minimum optimum spacing.)

For paths for which the level of the surface-reflected signal(s) is not expected to approach that of the direct signal in normal refractivity conditions (see § 6.1.2.4 and 6.1.2.5 to determine if this is the case), another design approach is possible. This is to choose one of the larger optimum spacings in equation (124) (e.g., $S_1 = 3\theta_1 / 2$ or $5\theta_1 / 2$) for the median value of k, such that it approaches, but is still less than S_1'. This will reduce the occurrence of surface multipath fading, but still give some significant space-diversity protection against it when it does occur. The advantage of decreasing the occurrence of surface multipath fading has to be weighed against the disadvantage of using a spacing that is not optimum over as large a range of effective k values (see Note 3).

As noted in § 2.2.2.2, some long paths (typically overwater) may occasionally require the use of three space diversity antennas. In this case the spacing between the upper and middle antennas should be the lowest possible optimum value from equations (124). The height of the lowest antenna should be based on the clearance rule in § 2.2.2.2 (see Note 4).

Step 8: paths without obvious specular surface reflections: Calculate the height of the diversity antenna from Steps 2-3 of § 2.2.2.2.

For the diversity antenna spacing obtained, carry out calculations of diversity improvement and outage using the methods of § 6.2.1 and 6.2.2. If the diversity spacing is greater than the $S = 23$ m limit of equation (124), perform the calculation with this limit since the actual improvement with the larger spacing would be greater. If necessary, calculate a new height for the upper antenna to satisfy outage criteria. In most cases, if the path clearance for the lower antenna has been chosen to minimize the occurrence of direct beam spreading and consequent surface multipath fading, it will not be necessary to increase the height of the upper antenna.

NOTE 1 – For two-leg passive reflector hops with one or more passive reflectors in close proximity, it is suggested that each leg be treated initially as an independent link for determining the spacing of diversity antennas at each end. If there are no obvious specular surface reflections, then the spacing determined for the longer leg should be employed also on the shorter leg.

NOTE 2 – These paths will mostly be those for which the surface reflected wave occurs on water and is not blocked in normal conditions, and the angle between the direct wave and the reflected wave at both antennas is within the 3 dB half width. Overland paths for which the reflection occurs on a very smooth land surface (e.g. wet or snow-covered plain) might also qualify.

NOTE 3 – It is considered that the advantage of decreasing the occurrence of surface multipath fading is the more important here. It is expected that when significant surface multipath fading does occur, it will be by virtue of a ground-based duct or otherwise extreme layer with a large negative gradient of refractivity located just below the path or partially below the path. Under these conditions, values of effective k less than the median will not be relevant. In any case, the estimated optimum spacing of the antennas should be based on the median effective k value.

NOTE 4 – If the spacing between the middle and lower antennas can be arranged to correspond to equations (124), with a small adjustment from the clearance rule of § 2.2.2.2, there may be some additional performance advantage to this.

6.2.2 Angular spacing in angle-diversity and combined space/angle-diversity systems

Angle diversity can be combined with space diversity to further enhance performance if desired. The space-diversity antennas are tilted to give this additional angle-diversity enhancement. The procedure for determining the tilt angles in either a space-diversity pair or a side-by-side angle-diversity pair is as follows:

Step 1: Tilt the main (upper) antenna of a space-diversity pair (or one of the antennas of a side-by-side angle-diversity pair) and the transmitting antenna upward by angles based on the procedures given in § 6.1.2.5 (see Note 1). This will result in a loss of flat fade margin in the approximate range 2.5 to 6 dB, the amount depending on whether the tilt is optimized to minimize fading or amplitude distortion. If necessary, use a larger antenna to compensate for the loss of flat fade margin entailed.

Step 2: Tilt the diversity (lower) antenna of a space-diversity pair (or the other antenna of a side-by-side angle-diversity pair) downwards from the local horizontal by an angle that is the lesser of:

– the angle in the direction of the dominant specular reflection along the path (under conditions of $k = \infty$); and

– the angle giving 3 dB of loss relative to boresight (see Note 2).

If there is more than one significant specular reflection along the path, a compromise pointing angle could be chosen. If there is no obvious specular reflection, an angle in the direction of the estimated strongest diffuse reflection (i.e. from terrain and/or vegetation) could be chosen. Otherwise, this antenna should be pointed in the direction of the line-of-sight in normal conditions, or the horizon if the line-of-sight is blocked.

NOTE 1 – It should be noted that the optimum tilt angles for transmitting and receiving antennas will not be the same unless the antenna heights above the surface reflection point along the path are identical. The larger tilt angle corresponds to the antenna with the larger angle in the direction of the surface reflection (see § 6.1.2.5).

NOTE 2 – The main objective here is twofold:

– to provide a combination of direct and surface reflected signal levels that is significantly different from that on the upper antenna so as to maximize the angle-diversity effect;

– to provide additional diversity protection in severe flat fading conditions due to beam spreading of the direct wave in one or more ducts along the path (i.e. the purposely enhanced surface-reflected signal is more likely to remain above the noise threshold in these situations).

The 3 dB limit is to avoid reducing the level of the direct signal on the diversity antenna by too much, particularly when the dominant specular reflection is in the foreground of the antenna.

Note that the resulting tilt angle may be positive with respect to the line-of-sight during normal conditions, particularly if the direct signal into the diversity antenna suffers significant diffraction loss during normal conditions (i.e. buried antenna).

6.2.3 Frequency separation in frequency diversity systems

The material in this section is included for those few situations where frequency diversity might be of value out of necessity, convenience, or perhaps in combination with space or angle diversity.

The appropriate frequency separation between main and protection channels in frequency diversity systems is governed by three factors:

– the system frequency plan available (see Series F, ITU-R Recommendations);

– the need to obtain a specified frequency diversity improvement factor for overland paths (see § 6.2.5.2);

– the desirability of minimizing the chance that the signal on one frequency will be faded at the same time as that on the other frequency is faded on highly reflective paths.

The step-by-step procedure to determine frequency separation is as follows:

Steps 1-4: Apply Steps 1-4 of § 6.1.2.3 to determine:

– if there are any path areas where a specular surface reflection might be significant; and

– if frequency diversity to combat surface multipath fading is necessary. If there are no significant surface specular reflection areas, go to Step 8.

Step 5: For the same range of effective k values in Step 3, calculate the minimum optimum frequency separation of main and protection channels from:

$$\Delta f_{min} = \frac{7.5 \times 10^4 \, d}{\left(h_1 - \frac{d_1^2}{12.74k} \right)\left(h_2 - \frac{d_2^2}{12.74k} \right)} \quad \text{MHz} \tag{125}$$

where h_1 and h_2 are in metres and d, d_1 and d_2 in kilometres. Carry out this step for each possible specular reflection area.

Step 6: Calculate the possible optimum frequency separations of main and protection channels from:

$$\Delta f = \Delta f_{min}, 3\Delta f_{min}, \text{etc.} \quad \text{MHz} \tag{126}$$

Again, carry out this step for each possible specular reflection area.

Step 7: paths with obvious specular surface reflections: For paths for which the level of the main surface-reflected signal is expected to approach that of the direct signal in normal refractivity conditions (i.e. median k or $k = 4/3$), the minimum optimum frequency separation obtained in Step 5 would be the ideal separation (see Note 1). This will give frequency diversity protection for the largest range of k values. Of course, the actual frequency separation will have to be a compromise between this ideal value and what is possible from the available frequency plan. Any changes from the ideal value to suit the frequency plan available should be in the direction of the minimum value obtained from equation (125) with $k = \infty$. However, it must be emphasized that the actual frequency separation need not equal the optimum value in order to obtain some frequency diversity protection. The method of § 6.2.5.2 can be used for guidance even for reflective paths.

For paths for which the level of the surface-reflected signal(s) is not expected to approach that of the direct signal in normal refractivity conditions (see § 6.1.2.4 and § 6.1.2.5 to determine if this is the case), another design approach may be possible in rare instances. This is to choose one of the larger optimum frequency separations in equation (126) for the median value of k if the frequency plan and the path parameters (such as unavoidably large antenna heights, h_1 and/or h_2, above the reflecting surface) allow this, or cross-band diversity is being employed. The disadvantage of using a frequency separation larger than the minimum optimum value is that it will not be as effective over as large a range of effective k values (see Note 2).

For hops with one or more passive repeaters giving two or more separate segments, equation (125) should be applied separately to the individual segments that have obvious specular reflections and the individual contributions added to obtain the total value of Δf_{min}. Those segments without an obvious specular reflection should be ignored in the summation.

Step 8: paths without obvious specular surface reflections: Carry out calculations of diversity improvement using the method of § 6.2.5.2, and adjust the frequency separation to minimize outage within the constraints of the frequency plan.

NOTE 1 – These paths will mostly be those for which the surface reflected wave occurs on water and is not blocked in normal conditions, and the angle between the direct wave and the reflected wave at both antennas is within the 3 dB half beamwidth. Overland paths for which the reflection occurs on a very smooth land surface (e.g. wet or snow-covered plain) might also qualify. In both cases, the smallest optimum separations occur for short paths with high antenna heights above the reflecting surface.

NOTE 2 – For paths with more than one significant surface-reflected signal, especially those for which levels are roughly comparable, some kind of compromise will have to be found between the various ideal frequency separations predicted and those available from the frequency plan. Again, it is emphasized that smaller than ideal frequency separations will allow some diversity protection.

6.2.4 Space-diversity improvement in narrow-band systems

The vertical space diversity improvement factor for narrow-band signals on an overland path can be estimated from:

$$I = \left[1 - \exp\left(-0.04 \times S^{0.87} f^{-0.12} d^{0.48} p_0^{-1.04} \right) \right] 10^{(A-V)/10} \tag{127}$$

where:

$$V = | G_1 - G_2 | \tag{128}$$

with:

A: fade depth (dB) for the unprotected path

p_0: multipath occurrence factor (%), obtained from equations (10) or (11)

S: vertical separation (centre-to-centre) of receiving antennas (m)

f: frequency (GHz)

d: path length (km)

G_1, G_2: gains of the two antennas (dBi).

Equation (127) was based on data in the data banks of Radiocommunication Study Group 3 for the following ranges of variables: $43 \le d \le 240$ km, $2 \le f \le 11$ GHz, and $3 \le S \le 23$ m. There is some reason to believe that it may remain reasonably valid for path lengths as small as 25 km. The exceedance percentage p_w can be calculated from equation (7) or (8), as appropriate. Equation (127) is valid in the deep-fading range for which equation (7) or (8) is valid.

6.2.5 Diversity techniques in digital systems

Methods are available for predicting outage probability and diversity improvement for space, frequency, and angle diversity systems, and for systems employing a combination of space and frequency diversity. The step-by-step procedures are as follows.

6.2.5.1 Prediction of outage using space diversity

In space diversity systems, maximum-power combiners have been used most widely so far. The step-by-step procedure given below applies to systems employing such a combiner. Other combiners, employing a more sophisticated approach using both minimum-distortion and maximum-power dependent on a radio channel evaluation may give somewhat better performance.

Step 1: Calculate the multipath activity factor, η, as in Step 2 of § 4.1.

Step 2: Calculate the square of the non-selective correlation coefficient, k_{ns}, from:

$$k_{ns}^2 = 1 - \frac{I_{ns} \times P_{ns}}{\eta} \tag{129}$$

where the improvement, I_{ns}, can be evaluated from equation (127) for a fade depth A (dB) corresponding to the flat fade margin F (dB) (see § 2.3.6) and P_{ns} from equation (29).

Step 3: Calculate the square of the selective correlation coefficient, k_s, from:

$$k_s^2 = \begin{cases} 0.8238 & \text{for} \quad r_w \le 0.5 \\ 1 - 0.195\,(1 - r_w)^{0.109 - 0.13 \log (1 - r_w)} & \text{for} \quad 0.5 < r_w \le 0.9628 \\ 1 - 0.3957\,(1 - r_w)^{0.5136} & \text{for} \quad r_w > 0.9628 \end{cases} \tag{130}$$

where the correlation coefficient, r_w, of the relative amplitudes is given by:

$$r_w = \begin{cases} 1 - 0.9746\,(1 - k_{ns}^2)^{2.170} & \text{for} \quad k_{ns}^2 \le 0.26 \\ 1 - 0.6921\,(1 - k_{ns}^2)^{1.034} & \text{for} \quad k_{ns}^2 > 0.26 \end{cases} \tag{131}$$

Step 4: Calculate the non-selective outage probability, P_{dns}, from:

$$P_{dns} = \frac{P_{ns}}{I_{ns}} \tag{132}$$

where P_{ns} is the non-protected outage probability given by equation (29).

Step 5: Calculate the selective outage probability, P_{ds}, from:

$$P_{ds} = \frac{P_s^2}{\eta\,(1 - k_s^2)} \tag{133}$$

where P_s is the non-protected outage probability given by equation (89).

Step 6: Calculate the total outage probability, P_d, as follows:

$$P_d = \left(P_{ds}^{0.75} + P_{dns}^{0.75} \right)^{4/3} \tag{134}$$

6.2.5.2 Prediction of outage using frequency diversity

The method given applies for a 1 + 1 system. Employ the same procedure as for space diversity, but in Step 2 use instead:

$$I_{ns} = \frac{80}{fd} \left(\frac{\Delta f}{f} \right) 10^{F/10} \tag{135}$$

where:

Δf: frequency separation (GHz). If $\Delta f > 0.5$ GHz, use $\Delta f = 0.5$

f: carrier frequency (GHz)

F: flat fade margin (dB).

This equation applies only for the following ranges of parameters:

$2 \le f \le 11$ GHz

$30 \le d \le 70$ km

$\Delta f / f \le 5\%$

6.2.5.3 Prediction of outage using angle diversity

Step 1: Estimate the average angle of arrival, μ_θ, from:

$$\mu_\theta = 2{,}89 \times 10^{-5}\, G_m\, d \qquad \text{degrees} \tag{136}$$

where G_m is the average value of the refractivity gradient (N-unit/km). When a strong ground reflection is clearly present, μ_θ can be estimated from the angle of arrival of the reflected ray in standard propagation conditions.

Step 2: Calculate the non-selective reduction parameter, r, from:

$$r = \begin{cases} 0.113 \sin\left[150\,(\delta/\Omega) + 30 \right] + 0.963 & \text{for} \quad q > 1 \\ q & \text{for} \quad q \le 1 \end{cases} \tag{137}$$

where:

$$q = 2505 \times 0.0437^{(\delta/\Omega)} \times 0.593^{(\varepsilon/\delta)} \tag{138}$$

and

δ: angular separation between the two patterns

ε: elevation angle of the upper antenna (positive towards ground)

Ω: half-power beamwidth of the antenna patterns.

Step 3: Calculate the non-selective correlation parameter, Q_0, from:

$$Q_0 = r \left(0.9399^{\mu_\theta} \times 10^{-24.58\,\mu_\theta^2} \right) \left[2.469^{1.879^{(\delta/\Omega)}} \times 3.615^{\left[(\delta/\Omega)^{1.978}(\varepsilon/\delta)\right]} \times 4.601^{\left[(\delta/\Omega)^{2.152}(\varepsilon/\delta)^2\right]} \right] \tag{139}$$

Step 4: Calculate the multipath activity parameter, η, as in Step 2 of § 4.1.

Step 5: Calculate the non-selective outage probability from:

$$P_{dns} = \eta\, Q_0 \times 10^{-F/6.6} \tag{140}$$

Step 6: Calculate the square of the selective correlation coefficient, k_s, from:

$$k_s^2 = 1 - \left(0.0763 \times 0.694^{\mu_\theta} \times 10^{23.3\,\mu_\theta^2} \right) \delta \left(0.211 - 0.188\,\mu_\theta - 0.638\,\mu_\theta^2 \right)^{\Omega} \tag{141}$$

Step 7: The selective outage probability, P_{ds}, is found from:

$$P_{ds} = \frac{P_s^2}{\eta\left(1 - k_s^2\right)} \tag{142}$$

where P_s is the non-protected outage (see Step 3 of § 5.1).

Step 8: Finally, calculate the total outage probability, P_d, from:

$$P_d = \left(P_{ds}^{0.75} + P_{dns}^{0.75} \right)^{4/3} \tag{143}$$

6.2.5.4 Prediction of outage using space and frequency diversity (two receivers)

Step 1: The non-selective correlation coefficient, k_{ns}, is found from:

$$k_{ns} = k_{ns,s}\ k_{ns,f} \tag{144}$$

where $k_{ns,s}$ and $k_{ns,f}$ are the non-selective correlation coefficients computed for space diversity (see § 6.2.5.1) and frequency diversity (see § 6.2.5.2), respectively.

The next steps are the same as those for space diversity.

6.2.5.5 Prediction of outage using space and frequency diversity (four receivers)

Step 1: Calculate η as in Step 2 of § 4.1.

Step 2: Calculate the diversity parameter, m_{ns}, as follows:

$$m_{ns} = \eta^3 \left(1 - k_{ns,s}^2\right) \left(1 - k_{ns,f}^2\right) \tag{145}$$

where $k_{ns,s}$ and $k_{ns,f}$ are obtained as in § 6.2.5.4.

Step 3: Calculate the non-selective outage probability, P_{dns}, from:

$$P_{dns} = \frac{P_{ns}^4}{m_{ns}} \tag{146}$$

where P_{ns} is obtained from equation (29).

Step 4: Calculate the square of the equivalent non-selective correlation coefficient, k_{ns}, from:

$$k_{ns}^2 = 1 - \sqrt{\eta} \left(1 - k_{ns,s}^2\right) \left(1 - k_{ns,f}^2\right) \tag{147}$$

Step 5: Calculate the equivalent selective correlation coefficient, k_s, using the same procedure as for space diversity (Step 3).

Step 6: The selective outage probability, P_{ds}, is found from:

$$P_{ds} = \left[\frac{P_s^2}{\eta\left(1 - k_s^2\right)} \right]^2 \tag{148}$$

where P_s is the non-protected outage probability given by equation (89).

Step 7: The total outage probability, P_d, is then found from equation (134).

7 Prediction of total outage

Calculate the total outage probability due to clear-air effects from:

$$P_t = \begin{cases} P_{ns} + P_s + P_{XP} \\ P_d + P_{XP} \end{cases} \quad \text{if diversity is used} \tag{149}$$

obtained by methods given in § 2.3.6, 4.1, 5.1, and 6.2.5.

The total outage probability due to rain is calculated from taking the larger of P_{rain} and P_{XPR} obtained by methods given in § 2.4.7 and 4.2.2.

The outage prediction methods given for digital radio systems have been developed from a definition of outage as BER above a given value (e.g. 1×10^{-3}) for meeting requirements set out in Recommendation ITU-T G.821. The outage is apportioned to error performance and availability (see Recommendations ITU-R F.594, ITU-R F.634, ITU-R F.695, ITU-R F.696, ITU-R F.697, ITU-R F.1092, ITU-R F.1189 and ITU-R F.557). The outage due to clear-air effects is apportioned mostly to performance and the outage due to precipitation, predominantly to availability. However, it is likely that there will be contributions to availability from clear-air effects and contributions to performance from precipitation.

8 Propagation aspects of bringing-into-service

In performing tests while bringing a system into service according to Recommendation ITU-R F.1330, it is desirable to avoid the times of year and times of day when multipath propagation is most likely to occur.

Studies carried out in eastern European temperate climates indicate that multipath propagation effects are least likely to occur in winter and in the two preceding months. For tests which must be carried out in summer, the period during the day when such effects were observed to be least likely was 1000-1400 h local time.

Measurements from a western European coastal climate at 60° North indicate that multipath propagation effects are least likely to occur 1300-2000 h local time regardless of the season. The winter period was the period least affected by fades caused by multipath propagation, followed by autumn and spring.

Appendix 1
to Annex 1

Method for determining the geoclimatic factor, *K*, from measured overland fading data

Step 1: Obtain the worst calendar month envelope fading distribution for each year of operation, using the long-term median value as a reference. Average these to obtain the cumulative fading distribution for the average worst month and plot this on a semi-logarithmic graph.

Step 2: From the graph note the fade depth, A_1, beyond which the cumulative distribution is approximately linear and obtain the corresponding percentage of time, p_1. This linear portion constitutes the large fade depth tail, which can vary by up to about 3 or 4 dB/decade in slope about the average "Rayleigh" value of 10 dB/decade, the amount of this variation depending on the number of years of data contained in the average distribution.

Step 3: Calculate the path inclination $|\varepsilon_p|$ from equation (6).

Step 4: Substitute the coordinates (p_1, A_1) of the "first tail point" into equation (7) or (8), as appropriate, along with the values $d, f, |\varepsilon_p|$ and calculate the geoclimatic factor, K.

Step 5: If data are available for several paths in a region of similar climate and terrain, or several frequencies, etc., on a single path, an average geoclimatic factor should be obtained by averaging the values of log K.

_____